THE ASTROPHYSICAL JOURNAL SUPPLEMENT SERIES, 113:311–331, 1997 December

HIGH-ENERGY SPECTRA OF ACTIVE GALACTIC NUCLEI. II. ABSORPTION IN SEYFERT GALAXIES

A. MALIZIA,[1] L. BASSANI,[1] J. B. STEPHEN,[1] G. MALAGUTI,[1] AND G. G. C. PALUMBO[1,2]
Received 1996 September 3; accepted 1997 May 29

ABSTRACT

Absorption by cold material in a large sample of active galaxies has been analyzed in order to study statistically the behavior of absorbed sources. The analysis indicates that on the basis of the column density alone, sources can be divided into low-absorption ($[N_H/N_{H_{Gal}}] \leq 50$) and high-absorption ($[N_H/N_{H_{Gal}}] \geq 50$) objects. While the second group consists mostly of narrow emission line galaxies (Seyfert galaxies of type 1.9–2), the first group is less homogenous, being formed by a mixture of broad and narrow emission line objects (Seyfert 1–2 galaxies). A study of the distribution of the column density values by means of bootstrap analysis confirms the reality of this effect. One group consisting of optically selected objects is well explained within the unified theory as nuclei obscured by a molecular torus. The second group made up of X-ray– and *IRAS*-selected objects is more difficult to define: in these sources the absorption is underestimated owing to difficulties (1) in fitting complex absorption spectra or (2) in measuring N_H values in Compton-thick sources or the absorption has a different origin than in the torus.

Possible correlations of absorption with X-ray luminosity, axial ratio, and Balmer decrement have also been investigated. Previous suggestions that lower luminosity AGNs tend to be more highly absorbed than those with higher luminosity are not confirmed by the present data; neither is any evidence for a correlation of N_H with axial ratio (b/a) found except for a preference of Seyfert 1–1.5 galaxies to be in face-on galaxies. While some sources (Seyfert 1–1.5 galaxies and low-absorption objects) have X-ray absorption compatible with Balmer decrement, high-absorption objects have column densities much higher than predicted from optical observations. These results are in agreement with the unified theory since the torus parameters are expected to be independent of luminosity, its orientation should be random with respect to the host galaxy, and its location should be in between the broad- and narrow-line regions. A study of the N_H variability indicates that in a large fraction (70%) of the sources for which the analysis could be done, N_H varies on timescales from months to years. In Seyfert 1–1.5 galaxies, the variability is associated with a region in or near the broad-line region and is explained in terms of partial covering and/or warm absorption models. In Seyfert 2 galaxies, the only variability observed is that associated with narrow emission line galaxies. The study of the column density distributions indicates that Seyfert 1–1.5 galaxies are characterized by $N_H = 18^{+9}_{-7} \times 10^{21}$ atoms cm^{-2}. Seyfert 1.9–2 galaxies have instead $N_H = 96^{+54}_{-35} \times 10^{21}$ atoms cm^{-2} and a larger dispersion; if this group is divided into low- and high-absorption objects, $N_H = 14.5^{+7.2}_{-5.3} \times 10^{21}$ atoms cm^{-2} and $N_H = 132.8^{+80.1}_{-52.6} \times 10^{21}$ atoms cm^{-2}, respectively, are obtained. The observed dispersion in each group is consistent with being entirely due to column density variability.

Subject headings: galaxies: active — galaxies: ISM — galaxies: Seyfert — X-rays: galaxies

1. INTRODUCTION

An interesting and strong feature that is found in the X-ray spectra of active galactic nuclei (AGNs) is the low-energy cutoff due to photoelectric absorption by cold or partly ionized material in the line of sight to the nucleus. The absorption effect due to our Galaxy, which has a column density $N_{H_{Gal}} \sim 3 \times 10^{20}$ atoms cm^{-2}, modifies the X-ray spectrum below $E < 0.6$ keV; anything observed above this energy is attributable to absorption in the active galaxy itself. The X-ray column density observed in different types of AGNs therefore undoubtedly contains important information about the distribution of matter around the nucleus. In hard X-ray–selected samples (see, e.g., Piccinotti et al. 1982), a significant fraction of all AGNs exhibits large column densities of cold material in the line of sight. For BL Lac objects (Ciliegi, Bassani, & Caroli 1995) and QSOs (Williams et al. 1992), the observed column densities are not dramatically different from galactic values, while Seyfert galaxies of all kinds can have values in excess of the galactic ones. More generally, all objects having quite high N_H values are generally associated with narrow emission line sources such as Seyfert 2 galaxies or narrow emission line galaxies (NELGs); the broad-line region in these objects may be hidden by surrounding material (Turner & Pounds 1989; Kruper, Urry, & Canizares 1990; Awaki 1991; Mushotzky, Done, & Pounds 1993). This is largely explained by the unified model in which these galaxies are viewed directly through a torus of obscuring material. In this scheme, large X-ray column densities may be due to the cold torus, the disk of the galaxy itself (Lawrence & Elvis 1982), or perhaps the broad-line clouds or material associated with the accretion disk.

Variations in the column density have been seen in a few objects widely known in the literature for their extremely high column density: NGC 4151 (Barr et al. 1977; Yaqoob & Warwick 1991; Yaqoob et al. 1993b), ESO 103-G35

[1] ITeSRE/C. N. R., Via P. Gobetti 101, 40129 Bologna, Italy; angela@tonno.tesre.bo.cnr.it.
[2] Dipartimento di Astronomia, Università di Bologna, Via Zamboni 33, 40126 Bologna, Italy.

(Warwick, Pounds, & Turner 1988), Centaurus A (Morini, Anselmo, & Molteni ; Turner et al. 1997), and NGC 5506 (Bond, Matsuoka, & Yamahuchi 1992). Although observations of high values of N_H ($\geq 10^{22}$) have been reported for a fraction of the AGNs observed at X-ray wavelengths, statistical studies of absorption have so far been based on instrument surveys (*EXOSAT*: Turner & Pounds 1989; *Einstein*: Kruper et al. 1990; and *Ginga*: Smith & Done 1996), which were limited to a small number of sources. The aim of the present work is to extend these studies by using a larger sample of objects based on data collected from the literature.

In § 2, the database is presented together with the criteria adopted to identify the absorbed objects. The sample obtained in this way is then used to investigate possible correlation of N_H with other parameters (§ 2), to study column density variations (§ 3), and to determine column density distributions for various classes of objects (§ 4). The final results are summarized in § 5.

2. SOURCE SELECTION

The sample of absorbed AGNs was selected using the high-energy ($E > 0.01$ keV) catalog of Malaguti, Bassani, & Caroli (1994), updated with measurements published up to July 1995 (see Tables 5 and 6 of the Appendix). The entire catalog, including new entries, contains 220 objects of various classifications excluding BL Lac objects, for a total of 1234 spectra. It includes 149 Seyfert galaxies (of which 82 are of type 1, 36 of type 2, 28 of intermediate type, and three of uncertain type), 66 quasars, and five objects otherwise classified. For completeness, both low-energy ($E < 2$ keV) spectra (in general, *Einstein* and *ROSAT* observations), as well as high-energy spectra ($E < 20$ keV) have been included in Table 6 of the Appendix; these data, however, have not been used in the present study. In order to be able to work on a large database and to be able to make a direct comparison between past and more recent observations, a simple representation of absorption (single neutral absorption fully covering the source) has been adopted in the present work. Recent observations, however, indicate that absorption in Seyfert galaxies is more complex than assumed here, especially when low-energy data are taken into account. Considerations of any effect introduced by this oversimplification will be addressed throughout the paper. In order to compare the observed values with absorption in our own Galaxy, values of galactic absorption along the line of sight to each source were extracted from either the *EXOSAT* Database and/or from the literature (see notes to Table 1 for details and the Appendix for references).

To extract sources with intrinsic absorption in excess of the galactic value, the average N_H for each object was calculated by weighting all available observations. Note, however, that the errors associated with N_H values were found to be asymmetric in the majority of cases, with positive errors often much greater than negative ones. The standard weighted mean analysis is not totally appropriate in this case, and therefore a Gaussian product method was used to determine a mean N_H value for each source. The method assumes that N_H corresponds to the most likely value of the column density, and that the errors e_u (upper) and e_l (lower) have Gaussian form on either side. Then, for a set of measurements N_{H_i}, one can calculate a probability distribution for the set of $P(N_H) = N \prod_i N_{H_i}$, where N is a normalization factor such that $\int_{-\infty}^{+\infty} P(N_H)\, dN_H = 1$. One can then take the maximum of this probability function to be the most likely value for the mean, $\bar{N}_H$, and integrate both above and below this value until $\int_{e_l}^{\bar{N}_H} P(N_H) dN_H = \int_{\bar{N}_H}^{e_u} P(N_H) dN_H = 0.32$, giving the 1 σ upper and lower errors, respectively. Obviously, if the set of measurements N_{H_i} is not well defined, so that, for example, there are two measurements incompatible with the source being constant and the errors being as quoted, then this method will fail, which indicates a problem with one assumption or other. This happened in only three occasions for NGC 3783, NGC 4151, and IC 4329A; of these three cases, only one observation was clearly incompatible with all others in the set, and so the weighted mean was calculated with this value removed. The difference between average $\langle N_H \rangle_A$ or weighted $\langle N_H \rangle_W$ values and the galactic absorption $N_{H_{Gal}}$ in the source direction was then evaluated in order to apply the following criteria as definitions of an absorbed source:

$$\langle N_H \rangle_W - N_{H_{Gal}} > 2\,\Delta N_H$$

$$\langle N_H \rangle_A - N_{H_{Gal}} > 2\sigma\ ,$$

where ΔN_H is the error and σ is its dispersion.

These criteria, when applied to the entire hard X-ray catalog, produced a sample of 45 absorbed objects, $\sim$20% of the 220 sources analyzed. Table 1 lists these objects together with their average and/or weighted mean absorption value, the error associated with the weighted mean (multiple data) or the average (single data point), and the dispersion as well as appropriate galactic absorption and AGN type. Except for a few objects (NGC 526A, NGC 4258, and NGC 2992), the classification has been taken from the NASA Extragalactic Database (NED). NGC 4258 has a LINER/Seyfert emission-line spectrum whose classification has long been debated (it is defined as type 1.5 in NED) until more recent data confirmed its Seyfert type 2 nature (Wilkes et al. 1995). NGC 526A is classified in NED as type 1.5, but it also belongs to the group of X-ray–selected NELGs (Mushotzky 1982) and, more recently, has been assigned the type 2 class by Whittle (1992). Both objects are here defined as type 2 Seyfert galaxies. NGC 2992 is here taken as a Seyfert galaxy of type 1.9 (Whittle 1992) instead of type 2. Finally, the radio galaxies Cen A and Cygnus A have been assigned class 2 as both are narrow-line emission galaxies.

The Seyfert 1 galaxies NGC 6814, 3A 0557−383, and the quasar NRAO 140, although objects with high N_H values, have been excluded from the present sample. In the first two cases, the source spectra may be contaminated by a nearby object (a galactic source for NGC 6814 [Madejski et al. 1993] and a BL Lac object for 3A 0557−383 [Giommi et al. 1989]), while in the third case, the line of sight to the source lies close to the Galactic plane ($b = -18.^\circ 8$) and behind the outer edge of a giant molecular cloud in Perseus (Ungerechts & Thaddeus 1987; Bania et al. 1991). The sources IRAS 04575−7537, IRAS 18325−5926, and Mrk 463E come from recently published data (not included in the Appendix): for the first two, N_H values have been taken from the work of Smith & Done (1996), while for Mrk 463E, the column density value come from a recent *ASCA* observation (Ueno et al. 1996). For a small number of sources, listed at the end of Table 1, only upper limits to the absorption are available (Awaki 1992; Awaki & Koyama 1993); given their Seyfert 2 classification, they are also discussed in

TABLE 1

SELECTED SAMPLE OF ABSORBED OBJECTS

Number (1)	Source (2)	N_H[a] Mean (N) (3)	N_H[a] W. Mean (N) (4)	Error (5)	Sigma (6)	$N_{H_{Gal}}$[a] (7)	Class (8)
1	III Zw 2	4.487 (6)	1.057 (3)	0.150	6.874	0.522[c]	Sey 1
2	Mrk 348	125.9 (1)	...	21.2[b]	...	0.578[c]	Sey 2
3	NGC 526A	17.433(9)	11.606 (7)	0.777	7.077	0.206[c]	Sey 2 (NELG)
4	Mrk 1040	26.25 (4)	3.581 (3)	1.047	35.652	0.705[c]	Sey 1.5
5	4U 0241+61	15.581 (7)	15.207 (6)	2.824	8.578	7.060[c]	Sey 1
6	NGC 1275	7.850 (2)	...	4.0[b]	...	0.144[c]	Sey 2
7	3C 111	10.274 (5)	14.255 (5)	0.900	6.952	2.820[c]	Sey 1
8	3C 120	2.278 (10)	1.931 (10)	0.131	0.996	1.080[c]	Sey 1
9	IRAS 04575−7537	10.5 (1)	...	2.9[b]	...	0.880[c]	Sey 2
10	NGC 1808	104.7 (1)	...	1.38[b]	...	0.247[c]	Sey 2
11	NGC 2110	32.458 (7)	24.941(7)	1.090	15.647	1.790[c]	Sey 2 (NELG)
12	Mrk 3	515.5 (2)	537.609 (2)	47.909	103.945	0.851[c]	Sey 2
13	PKS 0637−75	5.705 (2)	5.715 (2)	0.202	0.007	0.480[d]	QSO
14	IRAS 09104+4109	3.0 (1)	...	0.1	...	0.205[d]	Sey 2
15	NGC 2992	8.215 (15)	8.414 (15)	0.172	3.509	0.515[c]	Sey 1.9 (NELG)
16	MCG −5-23-16	14.255 (8)	16.046 (8)	0.742	5.508	0.883[c]	Sey 2 (NELG)
17	M81	10 (1)	...	2[b]	...	0.424[c]	Sey 1
18	NGC 3227	11.632 (12)	1.405 (12)	0.173	13.646	0.226[c]	Sey 1.5
19	IRAS 1040+706	147.9 (1)	...	1.35[b]	...	0.297[c]	Sey 2
20	NGC 3516	62.10 (9)	55.668 (5)	2.811	18.214	0.333[c]	Sey 1.5
21	NGC 3783	14.20 (8)	19.167 (8)	0.762	11.165	0.912[c]	Sey 1
22	NGC 4051	41.540 (11)	8.178(9)	1.342	72.058	0.131[c]	Sey 1
23	NGC 4151	73.756 (62)	66.961 (62)	1.097	26.075	0.204[c]	Sey 1.5
24	NGC 4258	150 (1)	...	20[b]	...	0.119[c]	Sey 2
25	NGC 4388	210 (1)	...	140[b]	...	0.261[c]	Sey 2
26	NGC 4507	490 (1)	...	70[b]	...	0.710[c]	Sey 2
27	NGC 4945	5370 (1)		500	...	0.983[f]	Sey 2
28	Cen A	125.769 (29)	128.067 (29)	0.347	38.694	0.700[d]	Sey 2 (RG)
29	MCG −6-30-15	4.631 (9)	1.400 (9)	0.168	3.738	0.427[c]	Sey 1
30	NGC 5252	30.850 (2)	29.551 (2)	17.626	10.394	0.204[c]	Sey 1.9
31	IC 4329A	3.611 (8)	3.337 (8)	0.138	1.723	0.440[c]	Sey 1
32	Mrk 463E	160 (1)	...	80	...	0.210[c]	Sey 2
33	NGC 5506	36.802 (14)	35.726 (14)	0.359	7.268	0.352[c]	Sey 1.9 (NELG)
34	NGC 5548	3.119 (18)	1.074 (14)	0.148	3.575	0.170[c]	Sey 1.5
35	NGC 5674	67.60 (1)	...	1.20[b]	...	0.240[c]	Sey 1.9
36	NGC 6552	870 (1)	...	180[b]	...	0.423[c]	Sey 2
37	IRAS 18325−5926	15.9 (1)	...	2.60[b]	...	0.750[c]	Sey 2
38	ESO 103−G35	183.375 (8)	233.938 (8)	7.677	73.89	0.580[d]	Sey 2 (NELG)
39	Cygnus A	375 (1)	...	71[b]	...	3.370[c]	Sey 2 (RG)
40	IC 5063	234.4 (1)	...	30.2[b]	...	0.436[g]	Sey 2
41	NGC 7172	98 (2)	105.733 (2)	4.936	11.314	0.163[c]	Sey 2 (NELG)
42	3C 445	114 (2)	98.585 (2)	28.403	86.267	0.515[c]	Sey 1
43	NGC 7314	8.467 (3)	7.890 (3)	0.488	4.406	0.146[c]	Sey 1.9
44	MRC 2251−178	0.827 (17)	0.866 (15)	0.066	0.368	0.273[c]	Sey 1
45	NGC 7582	169.043 (7)	93.197 (7)	6.817	147.221	0.148[h]	Sey 2 (NELG)
46	IRAS 01065−4644	<3.16 (1)	...	...	...	0.197[d]	Sey 2
47	NGC 1068	<5.0 (1)	...	...	...	0.457[d]	Sey 2
48	NGC 1672	6.31 (1)	...	<31.6	...	0.225[d]	Sey 2
49	NGC 1667	25.1 (1)	...	<100	...	0.627[d]	Sey 2
50	NGC 5643	<19.95 (1)	...	...	...	1.134[d]	Sey 2
51	IRAS 21116+0158	<15.85 (1)	...	...	...	0.582[d]	Sey 2
52	NGC 7674	<15.85 (1)	...	...	...	0.598[d]	Sey 2

NOTE.—(N) refers to the number of observations; Err and Sigma are the error and the dispersion of the weighted mean respectively; $N_{H_{Gal}}$ is the Galactic column density. Class terminology: Sey = Seyfert galaxy (number indicates type); RG = radio galaxy; QSO = quasar.

[a] In units of 10^{21} atoms cm^{-2}.

[b] Error on single measurement.

[c] Stark et al. 1990.

[d] *EXOSAT* database.

[e] Kruper, Urry, & Canizares 1990.

[f] $N_H = 10^{(-0.01393\times|bII|+21.1786)}$ Rowan-Robinson 1985.

[g] Dickey & Lockman 1990.

[h] Elvis , Lockman, & Wilkes 1989.

this work. There may be more absorbed sources like the high-redshift QSOs described by Wilkes et al. (1992), Elvis et al. (1994b), and Cappi et al. (1996) that were excluded because it is not yet clear what is the origin of the absorption, i.e., in the QSO itself or in intervening matter between the object and the observer. For all the above arguments, it turns out that the sample on which the present study is based contains, except for the quasar PKS 0637−75 and the radio galaxies Cen A and Cygnus A, only Seyfert galaxies.

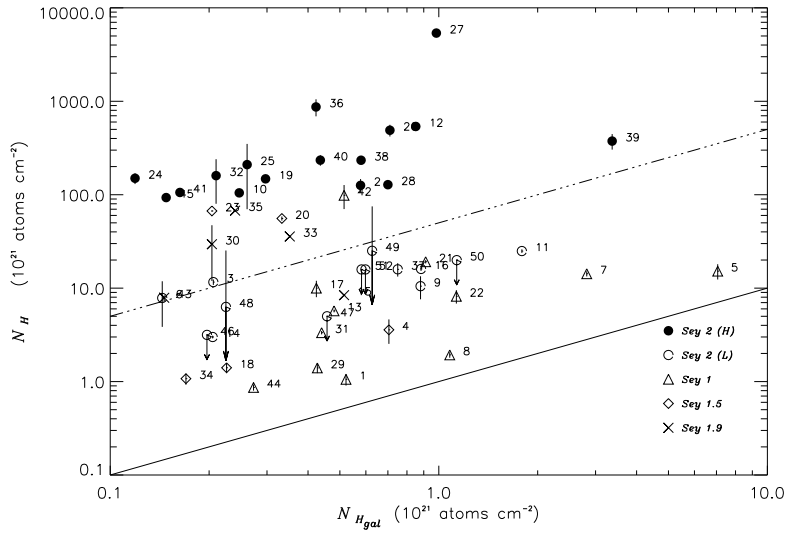

FIG. 1.—Plot of the column density values against galactic absorption in the source direction for all objects in Table 1 (here and in the following figures, sources are numbered as in Table 1). The solid line represents the one-to-one correspondence between N_H and $N_{H_{Gal}}$, while the dashed-dotted line highlights the division between low-absorption ($[N_H/N_{H_{Gal}}] \leq 50$) and high-absorption objects ($[N_H/N_{H_{Gal}}] \geq 50$).

Figure 1 is a plot of the N_H values of the selected sources compared to their relative galactic absorption. No data point lies below the one-to-one line correspondence, which confirms the effectiveness of the adopted source selection criteria. In this figure, as well as in the following ones, each source is characterized by its optical class and identified by the same number assigned in Table 1; note that the NELG classification has not been considered and that each object of this class has been assigned its proper Seyfert type, while the only QSO (PKS 0637−75) listed in Table 1 has been given the Seyfert 1 symbol.

An immediate and obvious conclusion that emerges from these results is that Seyfert 2 galaxies have almost invariably higher column densities than Seyfert 1 galaxies. This confirms previous results from *HEAO 1*, *EXOSAT*, and *Ginga* surveys and supports the hypothesis of a large obscuring region close to the center of Seyfert 2 galaxies, possibly hiding a Seyfert 1 nucleus, as suggested in the unified model of Antonucci & Miller (1985). Two main groups of objects are evident in Figure 1: one with $N_H/N_{H_{Gal}} < 50$ contains mostly Seyfert 1 and 1.5 galaxies, while the other with $N_H/N_{H_{Gal}} > 50$ is made of Seyfert 1.9 and 2 galaxies. A few exceptions are worth a note: a number of type 2 objects are found in the first group of sources, while the Seyfert 1 galaxy 3C 445 is located in the second group. While for 3C 445 the result may be surprising but is not significant given the uncertain definition of the source spectrum owing to contamination from a nearby cluster (Pounds 1990), for type 2 objects to be found in the first group is an unexpected result. However, one can argue that while high-absorption Seyfert 2 galaxies are mostly optically selected and easily explained as type 1 nuclei viewed through an obscuring torus, the low-absorption sources are either X-ray– (NELG) or infrared-(*IRAS*) selected objects. These bright X-ray galaxies do not show the high column densities expected in tori ($N_H > 10^{23}$), and yet their broad lines cannot be seen in the optical band. This discrepancy can be explained if in these sources the torus is still present but either it is either optically thin or our line of sight intercepts its rim; alternatively, in these sources the absorption has not been properly estimated or has a different origin than the torus. This point is discussed further in the next section. Seyfert galaxies of type 1.5 are present in both groups, which suggests that the same classification could be the result of different physical phenomena. In particular, NGC 4151 has been observed to have a variable H I profile over the past decades, being observed mostly as a Seyfert 1.5 galaxy but occasionally as a Seyfert 1.8 or 1.9 galaxy (Antonucci & Cohen 1983; Penston & Perez 1984). NGC 3516 is similar to NGC 4151 (Aoki et al. 1994; Kriss et al. 1996), while the other three objects (which are also often defined as type 1.2 in the literature; Whittle 1992) more closely resemble type 1 objects.

It is worth noting that the present sample extends the N_H values by at least an order of magnitude in comparison to previous samples (Turner et al. 1991; Nandra & Pounds 1994). This is mainly due to the inclusion of many Seyfert 2 galaxies in the sample. It is therefore justified a check on possible correlation between N_H and other parameters, listed in Table 2, as discussed in previous works, but underlying the behavior of different galaxy types.

In Figure 2, the N_H values of the selected sample sources are plotted against the corresponding $L_{(2-10)\,keV}$ averaged over all available observations and corrected for the appropriate absorption (Table 2, col. [6]). To provide a direct comparison with earlier works, a line is drawn at $10^{43.5}$ ergs s^{-1} to separate crudely the low- from the high-luminosity AGNs, while a line at $\sim 10^{22.2}$ atoms cm^{-2} is used to divide low from highly absorbed objects. The complete sample is divided in 28 low-luminosity and 23 high-luminosity objects; taking into consideration only highly absorbed objects, one finds 15 sources at low luminosities and 11 at high luminosities. Previous suggestions that lower luminosity AGNs tend to be more highly absorbed than higher luminosity ones (Mushotzky 1982; Lawrence & Elvis 1982; Reichert et al. 1985; Turner & Pounds 1989) are therefore not confirmed by the present data, especially if upper limits in the left-hand side of the graph are properly considered. This result is in agreement with the unified theory since the torus parameters such as optical thickness and opening angle are expected to be independent of luminosity. However, the lack of an anticorrelation between absorption

TABLE 2

INFORMATION ON THE SAMPLE'S OBJECTS

Number (1)	Source Name (2)	Redshift (z) (3)	b/a (4)	Flux[a] [2–10] keV (5)	Luminosity[b] [2–10] keV (6)	Hα/Hβ (7)	References for Hα/Hβ (8)
1	III Zw 2	0.089	1.00[c]	3.62	1242.43	3.63	1
2	Mrk 348	0.015	1.00	1.52	27.96	6.02	2
3	NGC 526A	0.019	0.53	2.70	45.96	3.00	2
4	Mrk 1040	0.016	0.21	2.07	23.37	6.60	1
5	4U 0241+61	0.044	...	3.57	334.03	16.22	3
6	NGC 1275	0.018	0.77	14.97	220.78	10.71	4
7	3C 111	0.049	...	3.30	380.42	...	...
8	3C 120	0.033	0.74	3.92	186.21	6.46	1
9	IRAS 04575...7537	0.018	1.00	2.25	34.30	>4.53	5
10	NGC 1808	0.003	0.60	0.56	0.38	14.17	6
11	NGC 2110	0.008	0.76	3.23	10.70	8.13	2
12	Mrk 3	0.013	0.89	0.62	22.14	6.61	2
13	PKS 0637−75	0.654	...	2.13	41030.78	...	...
14	IRAS 09104+4109	0.442	...	1.68	21047.5	...	...
15	NGC 2992	0.008	0.31	4.44	13.05	7.08	2
16	MCG −5-23-16	0.008	0.45	8.05	25.08	8.00	2
17	M81	[d]	0.52	0.70	0.04	7.60	7
18	NGC 3227	0.004	0.67	2.60	1.80	5.75	2
19	IRAS 1040+706	0.033[e]	...	0.73	68.80	7.20	f
20	NGC 3516	0.009	0.76	1.85	9.27	4.09	2
21	NGC 3783	0.004	0.89	40.85	32.53	3.70	2
22	NGC 4051	0.002	0.75	1.92	0.35	3.20	2
23	NGC 4151	0.003	0.71	16.38	9.62	3.10	2
24	NGC 4258	0.002	0.39	0.31	0.06	...	...
25	NGC 4388	0.008	0.26	1.86	14.11	5.89	2
26	NGC 4507	0.013	0.76	3.64	118.76	5.02	2
27	NGC 4945	0.002	0.19	0.84	408.50	...	...
28	Cen A	0.002	0.79	47.95	15.85	3.85	7
29	MCG −6-30-15	0.007	0.60	4.77	10.15	5.13	8
30	NGC 5252	0.023	0.64	0.87	24.66	3.72	9
31	IC 4329A	0.016	0.28	10.72	120.98	11.05	2
32	Mrk 463E	0.050	0.42[f]	0.28	219.42	5.62	2
33	NGC 5506	0.006	0.32	6.93	13.82	7.41	2
34	NGC 5548	0.017	0.93	4.11	51.43	4.20	2
35	NGC 5674	0.025	0.91	1.02	41.72	4.90	9
36	NGC 6552	0.026	0.70	2.35	6.00	...	...
37	IRAS 18325−5926	0.020	...	1.84	36.75	9.91	10
38	ESO 103−G35	0.013	0.36	2.38	44.81	12.06	2
39	Cygnus A	0.057	...	1.80	900.21	...	...
40	IC 5063	0.011	0.67	0.99	14.39	5.53	2
41	NGC 7172	0.009	0.56	3.03	18.74	6.50	7
42	3C 445	0.057	1.00[c]	1.21	292.54	9.12	i
43	NGC 7314	0.005	0.46	2.44	2.79	20.00	2
44	MCG 2251−178	0.068	...	2.73	545.69	5.62	1
45	NGC 7582	0.005	0.42	4.63	8.43	8.32	2
46	IRAS 01065−4644	0.031	0.67	1.0	42.07[g]	7.3	11
47	NGC 1068	0.004	0.84	0.67	0.42[g]	7.38	12
48	NGC 1672	0.004	0.83	0.30	0.26[g]	6.99	12
49	NGC 1667	0.015	0.83[c]	0.98	9.92[g]	9.74	12
50	NGC 5643	0.004	0.87	0.4	0.28[g]	5.58	12
51	IRAS 21116+0158	0.013	0.36	2.54	18.70[g]	...	...
52	NGC 7674	0.029	0.91	1.60	59.75[g]	5.00	2

NOTE.—All luminosities have been calculated assuming $H_0 = 50$ km s^{-1} Mpc^{-1} and $q_0 = 0$.

[a] Observed flux in units of 10^{-11} ergs cm^{-2} s^{-1}.

[b] Intrinsic luminosity in units of 10^{42} ergs s^{-1}.

[c] Kirhakos & Steiner 1990.

[d] Negative radial heliocentric velocity: $D = 3.5$ Mpc (Elvis & Van Speybroek 1982).

[e] De Grijp et al. 1992.

[f] Mazzarella & Boroson 1993.

[g] Uncorrected luminosity.

REFERENCES.—(1) Rudy 1984; (2) Mulchaey et al. 1994; (3) Morgan & Kwitter 1978; (4) Phillips, Charles, & Baldwin 1983; (5) De Grijp et al. 1992; (6) Véron-Cetty & Véron 1986; (7) Rebecchi et al. 1992; (8) Ward et al. 1988; (9) Osterbrock & Martel 1993; (10) WGACAT Database (High Energy Astrophysics Science Archive Research Center); (11) Kirhakos & Steiner 1990; (12) Storchi-Bergmann, Kinney, & Challis 1995.

and luminosity in the present study is not necessarily in contradiction with previous results since these were based primarily on Seyfert 1 data. Figure 2 indicates that in these sources there is a tendency for lower luminosity AGNs to be more highly absorbed, which indicates that the absorption is not torus related but is probably due to gas present outside the torus: higher ionization states of this gas for higher luminosities could well explain this trend. It is also

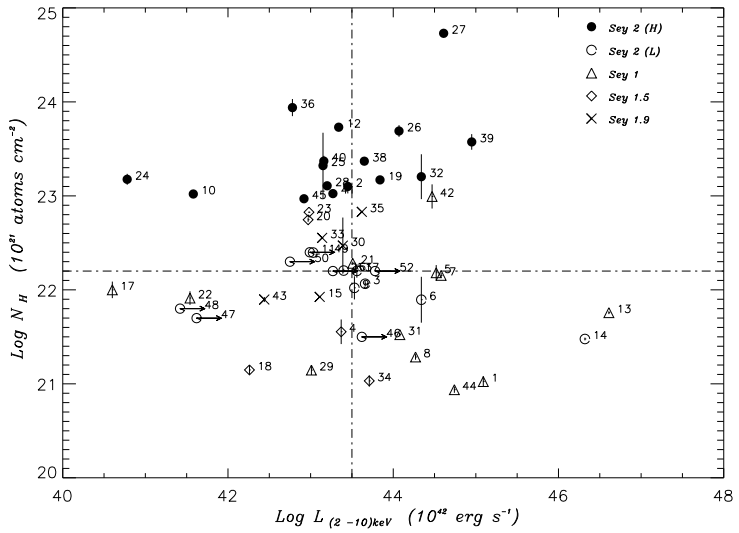

FIG. 2.—Plot of the absorption corrected luminosity vs. column density for all sample sources. The dividing lines correspond to $L_{[2-10]} = 10^{43.5}$ ergs s^{-1} and $N_H = 10^{22.2}$ atoms cm^{-2}, respectively.

interesting to note that the Seyfert 2 counterparts to the very luminous Seyfert 1 galaxies ($L_{(2-10)\,\mathrm{keV}} \sim 10^{45}$ ergs s^{-1}) are now found, thus removing a problem for the unified scheme of AGNs (Mulchaey, Mushotzky, & Weaver 1992).

Next, possible correlations of N_H values with the axial ratio (b/a) and Balmer decrement (Hα/Hβ) were investigated. Figure 3 shows the intrinsic column plotted against axial ratio (NED values). If the host galaxy ISM were the dominant absorbing material in AGNs, a correlation with inclination angle would be expected, and high columns would be observed only in objects seen close to edge-on ($b/a = 0$). Generally speaking, this is certainly not observed in the present sample whose objects are uniformly spread over the entire range of b/a values, nor there is any evident trend of this taking place in sources of the same optical type. As expected, there is a lack of unabsorbed objects seen edge-on, and it may be possible for a few sources that the absorption is partly due to the host galaxy (for example, in IC 4329A and Mrk 1040, but see the section on variability). The lack of any correlation indicates that the orientation of the X-ray–absorbing region relative to the line of sight is generally independent of the host galaxy orientation. Going into greater detail, we note that while there is a preference of Seyfert 1–1.5 galaxies to be found in face-on galaxies (only IC 4329A and Mrk 1040 have $b/a < 0.5$), Seyfert 2 galaxies are distributed over the whole range of b/a values, while intermediate Seyfert 1.9 galaxies are preferentially found in edge-on systems. The present result agrees with conclusions reached by Maiolino & Rieke (1995), who suggest that following McLeod & Rieke (1995) in Seyfert 2 galaxies, the X-ray absorption is related to an inner thicker torus independently oriented with respect to the host galaxy, while in Seyfert 1.9 galaxies, the absorbing region is supposed to be coplanar with the host galaxy and related to a thinner outer torus.

Figure 4 is a plot of X-ray absorption versus an optical reddening indicator such as the Balmer decrement; in the case of Seyfert 1 galaxies, this is mainly the broad-line ratio,

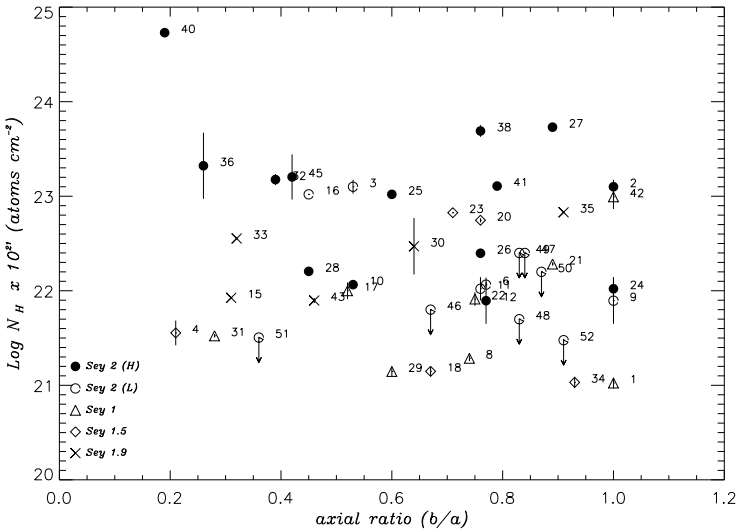

FIG. 3.—Plot of axial ratio versus column density for all sources in the sample; $b/a = 0$ and $b/a = 1$ correspond to edge-on and face-on galaxy disk geometry, respectively.

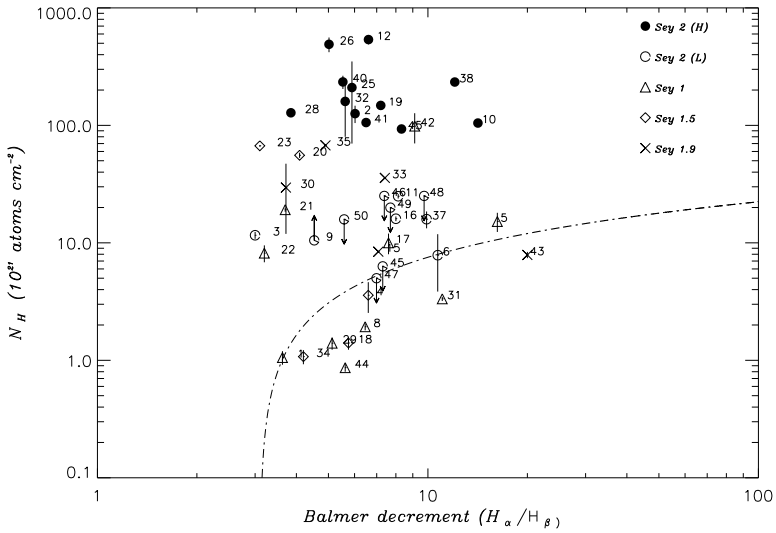

FIG. 4.—Plot of the Balmer decrement Hα/Hβ (broad-line ratio for Seyfert 1–1.5 galaxies and narrow-line ratio for Seyferts 1.9–2 galaxies) vs. column density for all sources in the sample. The dashed-dotted line represents the line of correspondence between visual extinction and X-ray absorption under the assumption of cosmic abundances, a dust-to-gas ratio appropriate for our own Galaxy, and photoionization due to a power law.

while for Seyfert 2 galaxies, it is the narrow-line ratio. Also shown in the figure is the line of correspondence between visual extinction and X-ray absorption under the assumption of cosmic abundances, a dust-to-gas ratio appropriate for our own Galaxy and photoionization due to a power law (Ward et al. 1987; Dahari & De Robertis 1988). Taking into consideration that the Balmer decrements are difficult to estimate and may be affected by variability and that also N_H may vary in time (see the next section), the extinctions inferred from column density measurements are in general agreement with those obtained from line observations for objects that are not heavily absorbed. These findings indicate that the absorbing material in these objects is probably located in the broad-line region (BLR)/narrow-line region (NLR) or still farther out. Most of these sources are Seyfert galaxies of type 1 and 1.5, while type 2 objects having N_H only slightly higher than predicted on the basis of Hα/Hβ belong to the NELG/*IRAS* class, i.e., to the group of objects having low absorption. For highly absorbed type 2 sources, the X-ray absorption is much higher than predicted from optical observations, which suggests that in these sources, the X-ray–absorbing region is not coincident with the narrow-line–producing region. Probably in these sources, the X-ray absorption occurs in a region located between the BLR (not observable) and the NLR (observable) and possibly associated with a torus as assumed in the unified theory of AGNs.

2.1. *Low-Absorption Seyfert 2 Galaxies*

Of the 35 Seyferts of type 1.9–2 present in the sample, 16 (14 of type 2 and only two of type 1.9) have $N_H/N_{HGal} \leq 50$, and as a consequence they are here classified as low-absorption Seyfert 2 galaxies. In particular, the sample consists of four NELGs (NGC 526A, NGC 2110, NGC 2992, and MCG −5-23-16), five *IRAS* galaxies (IRAS 04575−7537, IRAS 09104+4109, IRAS 18325−5926, IRAS 01065−4644, and IRAS 21116+0158), and seven other galaxies (NGC 1275, NGC 1068, NGC 1672, NGC 1667, NGC 5643, NGC 7314, and NGC 7674). NGC 1068 is a well-known example of a Compton-thick source, i.e., the emission is completely blocked by the obscuring torus, and the galaxy can be seen only via scattered/reflected emission. In this case, the source has a column density much higher than observed ($\geq 10^{25}$ cm^{-2}) and is erroneously classified as a low-absorption object. Also NGC 5643 and possibly IRAS 09104+4109 could be examples of Compton-thick sources as suggested by the detection of very strong iron lines in the *ASCA* spectra (Awaki 1997; Iwasawa 1994); in the case of NGC 5643, the measured value of the column density suggests also the existence of a second absorbing region. Also in NGC 2110 and NGC 2992, the absorption could be higher than reported here. For NGC 2110, *ASCA* data indicate the existence of two cold absorbing regions of column densities $\sim 10^{23}$ and $\sim 10^{22}$ atoms cm^{-2} corresponding to the BLR and the torus, respectively (Hayashi et al. 1996). For NGC 2992, the observation of a delay in the response of the Fe K line and Compton reflection to a decrease of the X-ray flux indicates the existence of a dense ($\sim 10^{24}$ atoms cm^{-2}) absorbing material identified as a molecular torus (Weaver et al. 1996); also in this case, a second absorbing region (possibly a dust lane) is inferred by the data. The other two NELGs could well be similar to NGC 2110 and NGC 2992 in that they also have spectral characteristics (hard X-ray spectra, weak iron line, and low absorption) which could be explained by the double absorber model (Smith & Done 1996). Although not X-ray–selected, NGC 7674 has X-ray characteristics that resemble those of NELGs (Awaki 1991) and therefore may be be associated with this type of galaxy.

The case of IRAS 18325−5926 differs, where the X-ray spectrum shows no evidence for cold and thick torus material; rather, the data indicate the presence of heavy obscuration globally covering the nucleus, including the broad- and narrow-line regions (Iwasawa 1994). This global obscuration picture may be related to the dusty nature of *IRAS*-selected galaxies, thus explaining their Seyfert 2 classification not in terms of the thick torus predicted by the unified scheme.

To conclude, while it is possible that some of the low-absorption Seyfert 2 galaxies can be recovered into the

high-absorption group, there is at least one case in which this is not possible; obviously, more X-ray data on the *IRAS*-selected objects may help in deciding if IRAS 18325-5926 is the exception or the rule.

3. VARIABILITY

To assess the presence of N_H variability, a χ^2 test was first applied to the data. This traditional method consists of calculating the residuals ΔN_{H_i} from the weighted mean $\overline{N_H}$ and comparing these values with the calculated errors. A reduced χ^2 of near unity indicates that the observations are compatible with a constant value, while much higher (or lower) values indicate either that the source is variable or that an assumption (usually in the magnitude of errors) is wrong. The results of the χ^2 test, applied to all those selected sources that have at least three X-ray spectra available, are summarized in columns (3), (4), and (5) of Table 3. For each source a number of interesting parameters are quoted: the χ^2 value obtained from the database ($\chi^2 = \Sigma_i[N_{H_i} - \overline{N_H}]^2/\sigma_i^2$, where σ_i are the 68% confidence measurement errors on N_{H_i} and $\overline{N_H}$ is the weighted mean of the column density of the source), the number of degrees of freedom (d.o.f.), and the χ^2 chance probability (P). The test shows that at a high confidence level ($P < 10^{-3}$), 17 of 23 sources that have more than three observations in the database show a variable column density.

The χ^2 method is not fully appropriate in the case of highly asymmetric errors; however, it is still possible to perform the same χ^2 analysis by substituting either the upper or lower error depending on whether the data point lies above or below the calculated mean. Unfortunately for points lying very close to the mean that have widely different upper and lower errors, this can lead to significantly different results arising from a very small difference in the calculated mean.

An alternative method was therefore necessary to cross-check variability results. The probability that N values, drawn from a population of mean and standard deviation unity, would have a maximum difference between two values of less than x [so for example as $x \to \infty$, $P(N, x) \to 1$] was calculated by Monte Carlo simulation and so produced the associated matrix $P(N, x)$. For each data set N_{H_i}, then, the difference $d_{i,j}$ in column densities between every pair of sources x_i, x_j was evaluated and expressed in terms of number of standard deviations, where the errors, above for the lower value and below for the higher measurement, were added in quadrature. The probability of a source being variable was then extracted from the matrix $P(N, x)$, where N is the number of measurements and x is the maximum of the set $d_{i,j}$. The probabilities obtained by applying this method are reported in Table 3 with the heading of maximum distance (MD) test.

It is clearly seen that the results of the two tests are in complete agreement; in fact, all 17 sources for which variability in N_H was obtained by the χ^2 test are also found to be variable by means of the MD method. For the two sources that were only marginally variable for the χ^2 test, under this test they are now found to be variable at the $\sim$90% level. The large percentage of variable sources found in the present sample contradicts previous evidence that indicates that variation of cold absorption in AGNs was a rare phenomenon (Mushotzky et al. 1993). It has been pointed out that a complex absorption component that is not variable but is measured by two instruments operating in different energy bands may give the appearance of variability (see the case of NGC 2992; Weaver et al. 1996). This possibility was investigated for each source found variable in Table 3. Data obtained over a broad energy band including a low X-ray energy coverage were either excluded or substituted with best-fit parameters obtained over a band encompassing

TABLE 3

RESULTS OF THE χ^2 AND MD TESTS FOR N_H VARIABILITY

		χ^2 TEST			MD TEST	
NUMBER (1)	SOURCE (2)	χ^2_ν (3)	d.o.f. (4)	P (5)	P(%) (6)	Variability (7)
1	III Zw 2	1.58	2	0.20	40.86	No
2	NGC 526A	1.94	6	0.07	37.19	No
3	Mrk 1040	1.44	2	0.24	49.63	No
4	4U 0241+61	1.37	5	0.23	36.05	No
5	3C 111	12.72	4	$<10^{-7}$	100	Yes
6	3C 120	5.38	9	2.38×10^{-7}	99.46	Yes
7	NGC 2110	7.63	6	$<10^{-7}$	99.99	Yes
8	NGC 2992	3.40	14	1.56×10^{-5}	99.36	[a]
9	MCG −5-23-16	8.48	7	$<10^{-7}$	99.98	Yes
10	NGC 3227	3.83	11	1.55×10^{-5}	84.46	[a]
11	NGC 3516	6.54	4	2.96×10^{-5}	99.14	Yes
12	NGC 3783	...	...	...	100	Yes
13	NGC 4051	9.95	8	$<10^{-7}$	99.73	Yes
14	NGC 4151	...	...	...	100	Yes
15	Cen A	18.75	28	$<10^{-7}$	100	Yes
16	MCG −6-30-15	14.07	8	$<10^{-7}$	100	Yes
17	IC 4329A	...	...	...	100	Yes
18	NGC 5506	5.72	13	$<10^{-7}$	99.88	Yes
19	NGC 5548	4.81	13	$<10^{-7}$	96.32	Yes
20	ESO 103−G35	7.11	7	$<10^{-7}$	99.56	Yes
21	NGC 7314	5.92	2	2.69×10^{-3}	91.14	Yes
22	MRC 2251−178	2.19	14	6.27×10^{-3}	89.98	Yes
23	NGC 7582	5.30	6	1.77×10^{-5}	97.12	Yes

[a] Yes, but see text for details.

only 2–10 keV (i.e., MPC and *EXOSAT* ME data were used instead of SSS + MPC and *EXOSAT* LE + ME data, respectively; unublished ME data have been fitted using the XSPEC package in order to estimate the new N_H value). The resulting data, which should not be effected by any bias due to instrument energy band, were again tested against variability using the DM test. At a level greater than 90%, absorption variability is confirmed for all sources except for NGC 2992 and NGC 3227. In the case of NGC 2992, variability is given only by one SSS + MPC measurement and disappears when this is replaced by the MPC best-fit absorption value; in agreement with Weaver et al. (1996), variability is probably an artifact owing to the energy band used. More complex is the case of NGC 3227, where variability is found at the 97.81% confidence level when only LE + ME data are used. Because in the energy band measured by these two instruments the spectrum is more complex than that above 2 keV (owing to the presence of various components, e.g., partial covering or warm absorber and soft excess), variability could result from a change in any of the spectral component present and not necessarily to a variation of the N_H value. For these reasons, variable absorption is not considered further in this source as in the case of NGC 2992. There is no correlation of N_H variability with AGN class: both type 1 and type 2 objects are found to be variable as are galaxies of intermediate type.

Dividing the variable sources into Seyfert 1 and Seyfert 2 galaxies, the intrinsic dispersion of absorption due to variability ranges from $\sigma = 0.37$ (MRC 2251−178) to $\sigma = 46$ (NGC 4051) for the first group and from $\sigma = 4.41$ (NGC 7314) to $\sigma = 147.22$ (NGC 7582) for the second one. An average dispersion σ of approximately 11 for Seyfert 1 galaxies (six if NGC 4051 is excluded) and 33 for Seyfert 2 galaxies is estimated; however, if this last group is divided into low- and high-absorption sources, then the values of σ is 6 and 79, respectively.

For a number of sources in the present sample, variability has already been discussed in the literature (see Table 4 for details and references), but for four sources (3C 111, MCG −5-23-16, NGC 3516, and NGC 7314), this is the first time that column density variations are reported. Note that IC 4329A, a source for which absorption has also been associated with the ISM of the host galaxy, is found variable. The present result indicates that at least part of the obscuring material in this source is located in a small region close to the nucleus. Short-term variability of N_H argues in favor of a localization of the absorbing material near the central source either in the BLR (Holt et al. 1980) or in the accretion disk (Lawrence & Elvis 1982), as these two regions are expected to produce variations on monthly timescales. On the other hand, owing to its position away from the nucleus and large-scale dimensions, the torus is expected to produce less pronounced variability and on a longer timescale (yearly). However, short-timescale sampling is rare, and much more data is required before any constraints can be put on the location of the absorbing region.

In one of the first scenarios proposed by Holt et al. (1980) for NGC 4151, one of the first sources found to be variable in N_H value, the X-ray absorption was associated with the same "cold" clouds that are responsible for the broad optical emission lines. In this scheme, the variability of absorption could arise from orbital motions that determine fluctuations in the number of clouds along the line of sight. Accordingly a lower limit to the timescale of variability is given by the time it takes a cloud to drift across and cover the source. Assuming a typical transverse velocity of 10,000 km s^{-1} typical of FWZI values of the emission lines from Seyfert 1 and Seyfert 2 galaxies, the time a cloud takes to cover the X-ray source (10^{15}–10^{16} cm in size) is $\sim$12 days; the most stringent constraints on Δt found in the case of NGC 4151 (about a week; Yaquoob, Warwick, & Pounds 1989) are fully compatible with the above estimate. More stringent is the constraint on the amplitude of the N_H change. Typically the source covering fraction is of the order of $>70\%$ (Reichert et al. 1985), which implies that 100 and more clouds are necessary to cover the X-ray source. The observed column densities (10^{22}–10^{23} cm^{-2}) infer a maximum thickness of a few clouds. It is difficult to explain a change by a factor of a few in column density as a Poisson variation in the number of clouds along the line of sight, and at least in one source, NGC 4151, this model has been rejected on the basis of the observational data (Yaqoob et al. 1993b).

An alternative explanation for the N_H variability is in terms of the warm absorption model, where variable absorption is due to a change in the ionization state of the material $\xi = L/nR^2$ (where L is the ionizing luminosity, R is the distance of the absorbing gas from the ionizing source, and n is the electron density). In this case the variability timescale may be as short as several hundred seconds (Halpern 1982), and therefore the present results are not restrictive. A number of possible causes could produce variation in U such as changes in luminosity, radial motion, or density. In particular, the observed ΔN_H could be due to luminosity variations of a factor of a few, which are quite common in Seyfert galaxies. Changes in the degree of

TABLE 4

SPECTRAL MODELS AND VARIABILITY REFERENCE INFORMATION

Source (1)	Warm Absorption (2)	Partial Covering (3)	Variability (4)
3C 111[a]			
3C 120			1, 2
NGC 2110	3	4	5, 6
MCG −5-23-16	3	8, 9	
NGC 3516	11	11	
NGC 3783	2, 3	7	12, 13
NGC 4051	3, 14, 15	16	8, 17
NGC 4151	18	19	4, 8, 20, 21
CEN A			8, 22, 23, 24
MCG −6-30-15	3, 8, 25	16	8, 26
IC 4329A	3, 17	27	28
NGC 5506		7, 8, 29	29
NGC 5548	3, 8, 30, 31, 32		30
ESO 103-G35			4, 8, 9, 33
NGC 7314[a]			
MRC 2251−178		34, 35	4, 15, 24, 34
NGC 7582		7	33

[a] Information on complex absorption not available.

REFERENCES.—(1) Kruper et al. 1990; (2) Turner et al. 1991; (3) Nandra & Pounds 1994; (4) Turner & Pounds 1989; (5)Weaver et al. 1995b; (6) Hayashi et al. 1996; (7) Reichert et al. 1985; (8) Mushotzky et al. 1993; (9) Mulchaey et al. 1993; (10) Ptak et al. 1994; (11) Kolman et al. 1993; (12) Mushotzky et al. 1980; (13) Hayes et al. 1981; (14) Mihara et al. 1994; (15) Pounds et al. 1994; (16) Matsuoka et al. 1990; (17) Fiore at al. 1992; (18) Yaqoob et al. 1989; (19) Holt et al. 1980; (20) Yaqoob & Warwick 1991; (21) Barr et al. 1977; (22) Morini et al. 1989; (23) Baity et al. 1981; (24) Halpern 1982; (25) Fabian et al. 1994; (26) Nandra, Pounds, & Stewart 1990; (27) Piro et al. 1990; (28) Singh et al. 1991; (29) Bond et al. 1992; (30) Nandra et al. 1991; (31) Nandra et al. 1993; (32) Kaastra 1991; (33) Warwick et al. 1993; (34) Pan et al. 1990; (35) Mineo & Stewart 1993.

photoionization as the continuum level varies also provide a natural explanation of the tendency of the X-ray spectrum to soften as the flux increases. As the flux of the central source increases, the ionization state of the absorber also increases, which reduces the opacity of the gas at low energies. This leads to an apparent change in the absorbing column density or softness ratio as a function of flux. For a number of variable sources, the $N_{\rm H}$ values were compared with their fluxes in order to investigate whether they were inversely correlated or not. Evidence for an inverse correlation was indeed found in 3C 120, NGC 4051, IC 4329A, NGC 7582, and possibly NGC 3516, but the result is not compelling, given the Pearson correlation coefficient r and the associated confidence C found ($0.7 < r < 0.9$, $78\% < C < 87\%$, except for NGC 3516, which gives a confidence of $\sim 60\%$).

It is interesting to note that a good fraction of the variable sources have in the literature spectra modeled either with a warm absorption or a partial covering model (see Table 4 for details). Recent *ASCA* observations of warm absorption edges tend to favor the warm absorption model. Combined with the present results, these measurements suggest that in Seyfert 1–1.5 galaxies, the association of the X-ray absorption with the warm ionized material near the nucleus is a viable possibility also in view of the observed variability, although some of these observations indicate that the data do not always match the prediction of the basic warm absorption model (Fabian et al. 1994; Otani et al. 1996).

The case of Seyfert 2 galaxies is different, where the absorption is believed to be associated with the torus, which should produce column density variations on longer timescales (a few years). Although no information is available on optically selected Seyfert 2 galaxies, $N_{\rm H}$ variability is a well-known characteristic of NELGs (only NGC 526A and NGC 2992 are not variable in the present sample).

Except for a couple of objects for which continuous monitoring allow to constrain the $N_{\rm H}$ variability timescale to the $\Delta t \leq$ months (~ 1 week for NGC 4151 and ~ 2 months for Cen A), for the majority of the analyzed objects, the only upper limit that can be set is of the order of 1 yr or more. While these findings are still compatible with the torus interpretation, shorter variability timescales need to be tested in order to put tighter restrictions on the location of the absorbing material in high $N_{\rm H}$ objects.

4. ABSORPTION DISTRIBUTION IN SEYFERT CLASSES

The absorption of objects of different classes in the present sample was next analyzed.

Figure 5 shows a histogram of the $N_{\rm H}$ values using weighted means whenever available or averages in the remaining cases as given in Table 1. A simple average of the column density values gives $N_{\rm H} = 221.93$ in units of 10^{21} cm^{-2} with an associated dispersion $\sigma = 802.58$, while the results obtained for the median and absolute dispersion are $N_{\rm H} = 32.45$ and $\sigma = 825.14$ (in the following, although omitted, all values are referred to the same units). An estimate of whether the observed spread is due only to measurement errors, σ_m or not, is obtained by calculating the ratio $\sigma^2/\langle\sigma_m^2\rangle$, which is expected to be around 1. Comparing the measurement errors with the dispersion values given above, a value of $\sigma^2/\langle{}^2_{\sigma_m}\rangle$ around 90 was obtained, which indicates an intrinsic spread in $N_{\rm H}$ values. This broad range of column density values is greater than expected from orientation effects, thus implying a range in torus parameters (thickness, optical depth, dimensions, etc.). Since in the previous section it was shown that a number of sources are characterized by a variable $N_{\rm H}$, the whole data set has been used in the following instead of mean values for each source. NGC 4151 and Cen A dominate the sample; in order to match the number of observations typically found for other objects, for both sources only a limited number of measurements have been used in the analysis. Recent observations have been favored with respect to older ones for their higher precision. The sample was then subdivided into the two main groups, Seyfert 1 and Seyfert 2 galaxies, and the above exercise was repeated. While the dispersion in type 1 objects was found to be rather low ($16 < \sigma < 29$), in type 2 sources it was found to be quite high ($138 < \sigma < 552$ or $85 < \sigma < 135$ if NGC 4945, the only object having $N_{\rm H}$ of the order of $\sim 10^{25}$, was excluded), which indicates that Seyfert 2 galaxies are mainly responsible for the large spread of $N_{\rm H}$ values observed in Figure 5.

An alternative method for estimating mean and intrinsic dispersion of the parent population is the maximum-likelihood (ML) method (Maccacaro et al. 1988; Worral 1989; Worral & Wilkes 1990). The results obtained for the above two groups are $\bar{N}_{\rm H_1} = 14^{+9.5}_{-8.5}$, $\sigma = 21^{+9}_{-6}$ and $\bar{N}_{\rm H_2} = 90^{+52}_{-50}$, $\sigma = 104^{+55}_{-33}$ (with the exclusion of NGC 4945), consistent with the results obtained above, together with

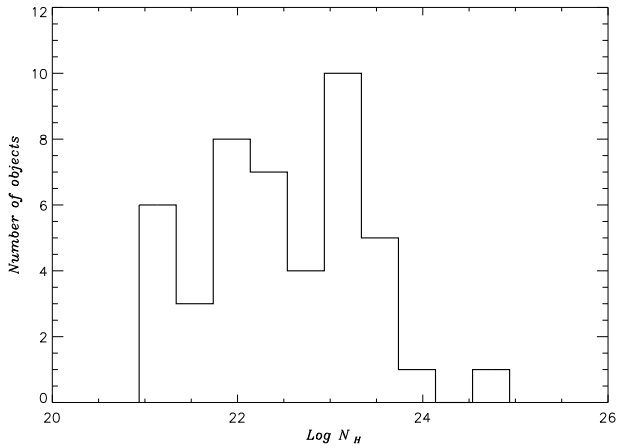

FIG. 5.—Histogram of the mean $N_{\rm H}$ values for those sources in Table 1 having a positive measurement of their column density

helpful information on the associated errors. However, since the ML analysis relies on the assumption that the data are normally distributed (which we do not known a priori), the samples were also tested with the Kolmogorov-Smirnov (K-S) test (Siegel & Castellan 1988). The K-S test clearly indicates that the observed N_H distributions cannot satisfactorily be represented by a Gaussian distribution. In spite of this, a Gaussian distribution of the parent population cannot be completely excluded. In fact, above 2 keV, the typical instrument sensitivity to absorption is limited to values greater than 10^{21}, while at high N_H values, a deficiency of sources may be due to the limited number of observations still available and/or limitation in the operational energy range of the instruments. Therefore the K-S test does not necessarily imply the inaccuracy of the ML method but indicates the need for a further test.

A different approach was then used in which the new nonparametric method of bootstrap sampling (Efron 1979, 1982) is applied to the data. With this method, many simulated data sets are obtained directly from the measured data. The simulated data sets, or "bootstrap samples," were then used to estimate the statistical variability in the parameter of interest, N_H in our case. A bootstrap sample is formed by selecting a subset of data from the available measurements by random resampling with replacement, i.e., one forms a bootstrap sample by randomly drawing from the set of measured data points without taking into account whether a point has already been selected or not. The only premise for the bootstrap technique is that the data contain all available information about the parent population.

The mean value of N_H and relative dispersion of the two groups on which a bootstrap sample of 10^6 data has been formed are respectively $\bar{N}_{H_1} = 18^{+9}_{-7}$, $\sigma = 28^{+14}_{-11}$ and $\bar{N}_{H_2} = 96^{+54}_{-35}$, $\sigma = 135^{+64}_{-68}$, in agreement with the ML analysis. These results are shown in Figure 6, where a clear bimodal distribution in N_H value is evident with Seyfert 1 galaxies occupying the lower corner and Seyfert 2 galaxies the upper corner of the plot. It is possible that selection effects that introduce a bias against intermediate N_H values can conspire to produce the observed class separation. For example, the adoption of a simple model (absorbed power-law) to describe the complexity of Seyfert spectra could have some effect. However, as the N_H values used herein are mostly obtained from fits utilizing data taken above 2 keV, such an effect should have a negligible influence on the distribution. For example, absorption results obtained using more complex models such as the warm absorption model are not much different from the N_H values used here (see Reynolds 1997 for a subsample of our sources) and so do not destroy the bimodality of the distribution displayed in Figure 6. Also, while it is true that more complex absorption models, such as those required by warm or partially covering absorption, tend to give for the same data set N_H values greater than those obtained with the simple model adopted here (for example, a neutral absorption of $N_H = 30$ corresponds in the warm absorption model to $N_H = 50$–60, depending on the ionization state of the absorber), it is equally true that given the validity of the same model for all sources, the data would be shifted and the gap maintained. Although it is never possible to exclude that other selection effects may have an impact on the data, it is difficult, however, to imagine a scenario in which such effects totally destroy the observed distribution; lacking strong observational evidence in such direction, it is assumed that the

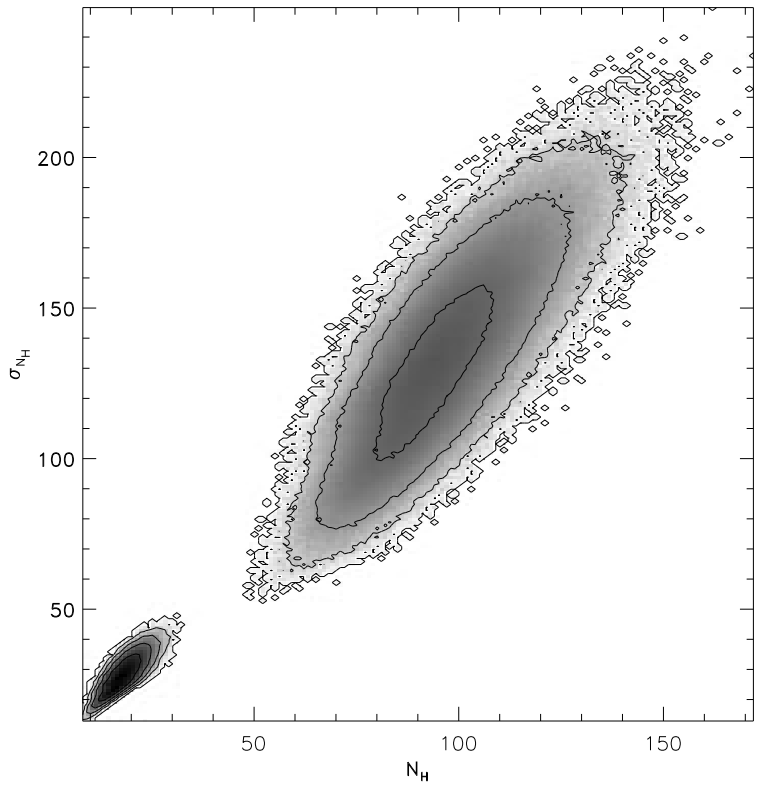

FIG. 6.—Distribution of the column density value and intrinsic dispersion obtained from the bootstrap method for Seyfert 1 galaxies (*lower corner*) and Seyfert 2 galaxies (*upper corner*); the contours do not correspond to confidence levels but rather to the most likely location of N_H and σ found by this method.

effect reported here is real. A possible way to interpret this result is by assuming a minimum column density for the torus and a maximum possible value of N_H in the line of sight to a Seyfert 1 galaxy. Then, as the viewing angle of the observer changes (going from a type 1 to a type 2 orientation), there will be a sudden increase in the column density, and only for a small range of inclination angles would intermediate columns be found.

The extremely small contours as well as the values of the population dispersion obtained for Seyfert 1 galaxies indicate that this class of objects is probably characterized by a small amount of absorption. This is even more evident if only strict Seyfert 1 galaxies are considered (see below). Furthermore, comparison with individual source data strongly indicates that most of the dispersion in this subsample can be due to the N_H variability. This result argues in favor of a similar material location and/or absorption mechanism, perhaps the warm absorber or partial covering as discussed in the previous section, common to this type of object.

On the contrary, type 2 objects are characterized by high absorption spreading over a large range of values. To verify this, the Seyfert 2 group was further subdivided into strict Seyfert 2 and intermediate type 1.9 galaxies, and the Seyfert 1 galaxies into Seyfert 1 and intermediate type 1.5 galaxies. The N_H and σ range for all four classes are, respectively, $1.38 < N_H < 9.2$ and $4.7 < \sigma < 21.4$ (Seyfert 1 galaxies, excluding 3C 445), $1.42 < N_H < 31.3$ and $27 < \sigma < 32.4$ (Seyfert 1.5 galaxies), $22 < N_H < 29$ and $14.3 < \sigma < 16.7$ (Seyfert 1.9 galaxies), and $78.4 < N_H < 132$ and $99.2 < \sigma < 152$ (Seyfert 2 galaxies with NGC 4945 excluded). As expected, Seyfert 1 and Seyfert 1.5 galaxies are different in column density values (mainly owing to the presence of NGC 4151 and NGC 3516 in this subsample), but surprisingly also Seyfert 1.9 and 2 galaxies are well separated in N_H and σ values: type 1.9 galaxies are characterized by a much smaller amount of absorption and a smaller dispersion than type 2 galaxies. This result would again be compatible with the existence of an outer thinner torus coplanar with the host galaxy and responsible for the intermediate type classification (Maiolino & Rieke 1995).

In view of the previous result the absorption distribution has also been studied by dividing the sample sources into three main groups: Seyfert 1–1.5 galaxies (excluding 3C 445, NGC 4151, and NGC 3516) and low-absorption and high-absorption Seyfert 2 galaxies (including type 1.9 objects). The results of the bootstrap analysis obtained in this case are shown in Figure 7. Low- and high-absorption objects are very well separated in the plot, again confirming the results of Figure 1. As discussed in § 2.1, this dichotomy could well be due to an underestimation of the absorbing column density values in these objects owing to their Compton thickness characteristics or to the limitations of fitting complex absorption with a simple model. Clearly, this point needs to be further studied as more data on the column density become available before accepting the reality of this separation effect.

As in Seyfert 1 galaxies, comparison with individual source data indicates that most of the dispersion observed in low-absorption objects can be due to N_H variability, keeping in mind the limitations discussed in § 2.1 for these objects. This is less evident for high-absorption objects: only for four objects in this class (Cen A, NGC 5506, NGC 7582, and ESO 103−G35) is there evidence of N_H varia-

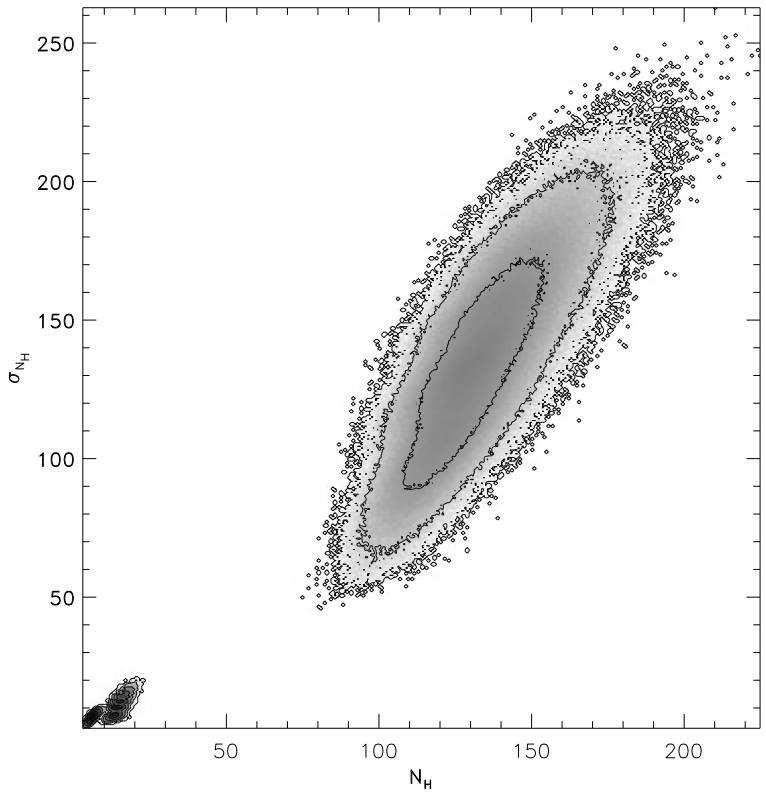

FIG. 7.—As in Fig. 6, but here the sample has been divided into three groups: Seyfert 1–1.5 galaxies (*lower corner, on the left*), low-absorption Seyfert 2 galaxies (*lower corner, on the right*), and high-absorption Seyfert 2 galaxies (*upper corner*).

tions. The observed dispersion in N_H values ranges from $\sigma = 7$ for NGC 5506 to $\sigma = 147.22$ for NGC 7582, with a mean value of $\sigma = 67$. Thus, although also in this case the N_H dispersion measured by the bootstrap method (50–250) is compatible with column density variations seen in individual objects, there may also be room for an intrinsic dispersion due either to an orientation effect or to differences in tori parameters. Indeed, more variability data on this type of objects are necessary to settle this issue.

5. CONCLUSIONS

Using a catalog of 1226 published high-energy spectra, a sample of 52 absorbed AGNs, all but one of which are Seyfert galaxies, has been selected, and on it, a statistical study of absorption effects in active galaxies has been attempted. The most important results of such analysis can be summarized as follows:

1. Absorption is common in Seyfert galaxies: typically 20% of sources with measured X-ray spectra have column density in excess of the galactic value.

2. With respect to absorption, active galaxies can be divided into two main groups: low-absorption and high-absorption objects. The first group comprises both broad and narrow emission line galaxies, while the second mainly contains narrow emission line objects. The first group can be further divided in Seyfert 1–1.5 galaxies and low-absorption Seyfert 2 galaxies. In Seyfert 1–1.5 galaxies, absorption tends to be related to material in the BLR; in highly absorbed objects, the absorption is probably associated with the torus. Less clear is the origin of the absorption in low absorbed Seyfert 2 galaxies. In these sources, either the column density is underestimated, thus indicating that they too contain a thick torus, or the absorption is not torus related, thus indicating the possible existence of a different type of Seyfert 2 galaxy.

3. No significant correlation of N_H with luminosity, axial ratio, or Balmer decrement has been found, which implies that the absorption in tori is independent from these parameters.

4. A large fraction ($\sim 70\%$) of the sources analyzed show variable column density. The variability is compatible within each group with the presumed location of the absorbing material.

5. The study of the N_H distributions in various subsamples indicate that while Seyfert 1–1.5 galaxies and low-absorption Seyfert 2 galaxies have a mean of N_H of $\simeq (1\text{–}2) \times 10^{22}$ cm^{-2} and a small dispersion around these values, high-absorption objects are characterized by a mean N_H of $\sim 10^{23}$ cm^{-2} and a larger dispersion. Furthermore, the observed dispersion can be due to absorption variability.

The complete catalog is available in computer readable form (ASCII file). Copies can be requested from A. Malizia (Istituto TESRE/CNR, via P. Gobetti 101, 40129 Bologna, Italy).

A. M. acknowledges CNR for a fellowship and N. Mandolesi for the hospitality at the TeSRE Institute. She also thanks G. Di Cocco for his continuous support. Thanks are also due to M. Polletta and M. Cappi for useful discussions and comments. The referee is thanked for a very careful reading and useful comments that improved the quality of the paper. This research has made use of data obtained through NASA/IPAC Extragalactic Database (NED) which is operated by the Jet Propulsion Laboratory, Caltech, under contract with the National Aeronautics and Space Administration; the High Energy Astrophysics Science Archive Research Center Online Service, provided by NASA-Goddard Space Flight Center; the SIMBAD database, operated at CDS, Strasbourg, France; and the European Space Information System (ESIS), located at ESRIN, Italy in the Information System Division of the European Space Agency. Financial support from MURST, CNR, and ASI is gratefully acknowledged.

APPENDIX

In this appendix we present an update of the catalog of high-energy spectra of AGNs by Malaguti et al. (1994). As in the main catalog, we have limited the search to a low-energy threshold of $E = 0.01$ keV and have collected spectra up to 40 keV. Since the main purpose of the present work was to create a sample of absorbed objects, we have neglected BL Lac objects. We have gathered 204 new spectra corresponding to 73 objects, which include 60 Seyfert galaxies (25 of type 1, 20 of type 2, and 15 of intermediate type), 10 quasars, and two radio galaxies. Of these 73 objects, 11 are new detections and therefore are not present in the previous catalog. Table 5 lists optical position, redshift, AGN class, and galactic hydrogen column density in the source direction for all 73 sources. For each object, all these values have been taken from the sources quoted; the class terminology is given in a footnote to the table.

The update of the catalog itself is presented in Table 6, which contains all spectral data and associated information. Some of the new spectra, mainly from *Ginga* observations, do not correspond to new observations but are the result of a reanalysis of the same data set previously published. The dagger (†) beside the source name in Table 6 indicates the updating of one or more *Ginga* observations. Accordingly with the previous catalog, we report only spectral fit parameters obtained assuming a power-law model corrected for cold gas absorption along the line of sight: photon index, 1 keV intensity in photons cm^{-2} s^{-1} keV^{-1} (which corresponds to 662.691 μJy) and, whenever available, the column density value (this corresponds sometimes just to the value of N_H in our galaxy). All the quoted parameters are given together with their associated errors and the corresponding confidence level. In Table 6 are reported the source name (col. [2]), the reference from which the spectrum has been taken (col. [3]), the instrument that made the observation (col. [4]), the energy band (in keV) over which the spectral fit was performed (col. [5]), the date of the observation (col. [6]), the spectral fit parameter with their associated errors (photon index (col. [7]), 1 keV intensity (col. [8]), hydrogen column density in cm^{-2} (col. [9]), and the statistical parameters that quantify the goodness of the fit (reduced χ^2 (col. [10]), the number ν of degrees of freedom (col. [11]), and the confidence level (in percentage) of the quoted errors (col. [12]). A three-dot ellipsis indicates that the relevant entry was either not considered in the fit or not reported in the quoted reference.

TABLE 5

AGNs IN THE CATALOG

Number (1)	Source (2)	α_{1950}[a] (3)	δ_{1950}[a] (4)	Class (5)	z[a] (6)	$N_{H_{Gal}}$[b] (7)
1	Mrk 335	00 03 45.2	+19 55 29	Sey 1[a]	0.026	0.410[c]
2	S5 0014+81	00 14 04.4	+81 18 29	QSO[a]	3.380	1.350[c]
3	Mrk 348	00 46 04.9	+31 41 05	Sey 2[a]	0.015	0.580[d]
4	NGC 526A	01 21 38.0	−35 19 42	Sey 1.5[a]	0.019	0.233[e]
5	Fairall 9	01 21 51.0	−59 03 54	Sey 1[a]	0.047	0.284[f]
6	Mrk 573	01 41 22.9	+02 05 56	Sey 2[a]	0.017	0.300[d]
7	NGC 985	02 32 10.5	−09 00 22	Sey 1.5[g]	0.043	0.283[f]
8	ESO 198−G24	02 36 40.7	−52 24 29	Sey 1[a]	0.045	0.300[d]
9	NGC 1068	02 40 07.1	−00 13 31	Sey 2[a]	0.004	0.310[d]
10	Mrk 372	02 46 31.4	+19 05 50	Sey 1.5[a]	0.031	0.930[d]
11	NGC 1275	03 16 29.6	+41 19 52	Sey 2[a]	0.018	1.520[c]
12	NGC 1365	03 31 41.0	−36 18 24	Sey 1[a]	0.006	0.140[d]
13	NRAO 140	03 33 22.4	+32 08 37	QSO[a]	1.258	1.200[c]
14	3C 111	04 15 00.4	+37 54 16	Sey 1[a]	0.049	3.261[e]
15	3C 120	04 30 31.6	+05 15 00	Sey 1[a]	0.033	1.232[e]
16	PKS 0438−43	04 38 43.2	−43 38 54	QSO[a]	2.852	0.150[h]
17	NGC 1672	04 44 55.0	−59 20 18	Sey 2[a]	0.005	0.520[d]
18	NGC 1667	04 46 10.5	−06 24 24	Sey 2[a]	0.015	0.517[c]
19	IRAS 04575−7537	04 57 36.0	−75 37 00	Sey 2[a]	0.018	0.519[i]
20	NGC 1808	05 05 58.6	−37 34 36	Sey 2[a]	0.003	0.247[c]
21	Akn 120	05 13 37.9	−00 12 15	Sey 1[a]	0.031	1.130[f]
22	Pic A	05 18 23.6	−45 49 43	Sey 1[a]	0.035	0.550[d]
23	NGC 2110	05 49 46.4	−07 28 02	Sey 2[a]	0.008	1.860[e]
24	MCG 8-11-11	05 51 09.6	+46 25 51	Sey 1[a]	0.021	2.027[e]
25	Mrk 3	06 09 48.4	+71 03 11	Sey 2[a]	0.013	1.810[d]
26	Mrk 78	07 37 56.8	+65 17 42	Sey 2[a]	0.037	0.390[d]
27	Mrk 79	07 38 47.3	+49 55 41	Sey 1.2[a]	0.022	0.589[e]
28	3C 212	08 55 55.5	+14 21 24	QSO[j]	1.049	0.370[c]
29	NGC 2992	09 43 17.7	−14 05 43	Sey 2[a]	0.008	0.556[e]
30	MCG −5-23-16	09 45 28.4	−30 42 57	Sey 2[a]	0.008	0.850[c]
31	M81	09 51 27.3	+69 18 08	Sey 1[a]	[k]	0.450[c]
32	M82	09 51 42.9	+69 55 00	SB[l]	0.001	0.420[c]
33	NGC 3227	10 20 46.8	+20 07 06	Sey 1.5[a]	0.004	0.220[d]
34	IRAS 1040+706	10 40 32.1	+70 40 04	Sey 2[a]	0.033[m]	0.297[c]
35	NGC 3516	11 03 22.8	+72 50 20	Sey 1.5[a]	0.009	0.300[d]
36	NGC 3783	11 36 33.0	−37 27 42	Sey 1[a]	0.011	0.923[f]
37	NGC 4051	12 00 36.4	+44 48 35	Sey 1[a]	0.002	0.131[e]
38	NGC 4151	12 08 01.0	+39 41 02	Sey 1.5[a]	0.003	0.210[d]
39	NGC 4258	12 16 29.4	+47 34 53	Sey 1[a]	0.0015	0.120[n]
40	3C 273	12 26 33.2	+02 19 43	QSO[a]	0.158	0.177[f]
41	NGC 4593	12 37 04.6	−05 04 11	Sey 1[a]	0.008	0.197[e]
42	3C 279	12 53 35.8	−05 31 08	QSO[a]	0.538	0.222[e]
43	NGC 4945	13 02 31.0	−49 12 12	Sey 2[a]	0.002	0.983[h]
44	MCG −6-30-15	13 33 01.8	−34 02 27	Sey 1[a]	0.007	0.406[e]
45	NGC 5252	13 35 44.4	+04 47 47	Sey 1.9[a]	0.023	0.197[o]

TABLE 5—*Continued*

Number (1)	Source (2)	α_{1950}[a] (3)	δ_{1950}[a] (4)	Class (5)	z[a] (6)	$N_{H_{Gal}}$[b] (7)
46	Mrk 273	13 42 51.7	+56 08 14	Sey 2[a]	0.038	0.100[d]
47	IC 4329A	13 46 27.0	−30 03 41	Sey 1[a]	0.016	0.455[e]
48	Mrk 279	13 51 53.6	+69 33 13	Sey 1[a]	0.029	0.164[e]
49	Mrk 464	13 53 45.4	+38 49 07	Sey 1.5[a]	0.051	0.110[c]
50	NGC 5506	14 10 39.1	−02 58 26	Sey 1.9[a]	0.006	0.422[e]
51	NGC 5548	14 15 43.5	+25 22 01	Sey 1.5[a]	0.017	0.193[f]
52	NGC 5674	14 31 22.5	+05 40 38	Sey 1.9[a]	0.025	0.240[d]
53	Mrk 478	14 40 04.5	+35 39 07	Sey 1[a]	0.079	0.097[f]
54	Mrk 841	15 01 36.3	+10 37 56	Sey 1[a]	0.036	0.233[e]
55	3CR 345	16 41 17.6	+39 54 11	QSO[a]	0.593	0.074[e]
56	4C 34.47	17 21 32.0	+34 20 42	QSO[a]	0.206	0.306[e]
57	NGC 6552	18 00 08.0	+66 36 54	Sey 2[a]	0.026	0.423[c]
58	QSO 1821+643	18 21 41.9	+64 19 01	QSO[a]	0.297	0.410[f]
59	3C 382	18 33 12.0	+32 39 18	Sey 1[a]	0.058	0.785[f]
60	ESO 103−G35	18 33 22.0	−65 28 18	Sey 2[a]	0.013	0.580[c]
61	3C 390.3	18 45 37.6	+79 43 07	Sey 1[a]	0.056	0.408[f]
62	ESO 141−G55	19 16 57.0	−58 45 54	Sey 1[a]	0.036	0.495[f]
63	Cygnus A	19 57 44.4	+40 35 46	RG[a]	0.057	2.400[p]
64	Mrk 509	20 41 26.3	−10 54 18	Sey 1[a]	0.034	0.399[f]
65	H2106−099	21 06 28.0	−09 52 30	Sey 1.2[a]	0.027	0.496[c]
66	PKS 2126−15	21 26 26.7	−15 51 52	QSO[a]	3.266	0.485[e]
67	NGC 7172	21 59 07.6	−32 06 42	Sey 2[a]	0.009	0.165[e]
68	NGC 7213	22 06 08.4	−47 24 45	Sey 1[a]	0.006	0.194[f]
69	NGC 7314	22 33 00.0	−26 18 36	Sey 1.9[a]	0.005	0.145[e]
70	Akn 564	22 40 18.3	+29 27 47	Sey 1[a]	0.024	0.634[f]
71	NGC 7469	23 00 44.4	+08 57 20	Sey 1[a]	0.016	0.482[e]
72	MCG −2-58-22	23 02 07.1	−08 57 20	Sey 1.5[a]	0.047	0.366[f]
73	NGC 7582	23 15 38.0	−42 38 36	Sey 2[a]	0.005	0.148[e]

NOTES.—Units of right ascension are hours, minutes, and seconds, and units of declination are degrees, arcminutes, and arcseconds. Class terminology: Sey = Seyfert galaxy (number indicates type); RG = radio galaxy; QSO = quasar.

[a] NASA Extragalactic Database.
[b] In units of 10^{21} atoms cm^{-2}.
[c] *EXOSAT* database.
[d] Kruper, Urry, & Canizares 1990.
[e] Elvis et al. 1989.
[f] Walter & Fink 1993.
[g] Hewitt & Burbidge 1991.
[h] Wilkes et al. 1992.
[i] $N_H = 10^{(-0.01393 \times |b^{II}| + 21.1786)}$; Rowan-Robinson 1985.
[j] Elvis et al. 1994b.
[k] Negative radial heliocentric velocity: $D = 3.5$ Mpc (Elvis & Van Speybroek 1982).
[l] Elvis & Van Speybroek 1982.
[m] De Grijp et al. 1992.
[n] Fabbiano et al. 1992.
[o] Dickey & Lockman 1990.
[p] Djorgovski et al. 1991.

REFERENCES

Antonucci, R. R. J., & Cohen, R. D. 1983, ApJ, 271, 564
Antonucci, R. R. J., & Miller, J. S. 1985, ApJ, 297, 621
Aoki, K., Othani, H., Yoshida, M., & Kosugi, G. 1994, PASJ, 46, 539
Awaki, H. 1991, Ph.D. thesis, Nagoya Univ.
———. 1992, in Proc. of Frontiers of X-Ray Astronomy, ed. Y. Tanaka & K. Koyama (Tokyo: Universal Academy), 537
———. 1997, in ASP Conf. Proc. 113, Emission Lines in Active Galaxies, ed. B. M. Peterson, F. Z. Cheng, & A. S. Wilson
Awaki, H., & Koyama K. 1993, Adv. Space Res., 13(12), 221
Baity, W. A., et al. 1981, ApJ, 244, 429
Bania, T. M., Marscher, A. P., & Barvanis, R. 1991, AJ, 101, 6
Barr, P., White, N. E., Sanford, P., & Ives, J. C. 1977, MNRAS, 181, 43
Bond, I., Matsuoka, M., & Yamahuchi, M. 1992, ApJ, 405, 179
Brandt, W. N., Fabian, A. C., Nandra, K., Reynolds, C. S., & Brinkmann, W. 1994, MNRAS, 271, 958
Brandt, W. N., Fabian, A. C., Nandra, K., & Tsuruta, S. 1993, MNRAS, 265, 996
Brinkmann, W., & Siebert, J. 1994, A&A, 285, 812
Cappi, M., Mihara, T., Matsuoka, M., Brinkmann, W., Prieto, M. A., & Palumbo, G. G. C. 1996, ApJ, 456, 141
Ciliegi, P., Bassani, L., & Caroli, E. 1995, ApJ, 439, 80
Dahari, O., & De Robertis, M. M. 1988, ApJS, 67, 249
De Grijp, M. H. K., Keel, W. C., Miley, G. K., Godfrooij, P., & Lub, J. 1992, A&AS, 96, 389
Dickey, J., & Lockman, F. J. 1990, ARA&A, 28, 215
Djorgovski, S., Weir, N. Matthews, K., & Graham, J. R. 1991, ApJ, 372, 67
Efron, B. 1979, Rietz Lecture Ann. Statistics, 7, 1
———. 1982, The Bootstrap, Jackknife, and Other Resampling Plans (Philadelphia: SIAM)
Elvis, M., Fiore, F., Mathur, S., & Wilkes, B. J. 1994a, ApJ, 425, 103
Elvis, M., Fiore, F., Wilkes, B., McDowell, J., & Bechtold, J. 1994b, ApJ, 422, 60
Elvis, M., Lockman, F. J., & Wilkes, B. J. 1989, AJ, 97, 777
Elvis, M., Matsuoka, M., Siemiginowska, A., Fiore, F., Mihara, T., & Brinkmann, W. 1994c, ApJ, 436, 55
Elvis, M., & Van Speybroek, L. 1982, ApJ, 286, 144
Fabbiano, G., Kim, D.-M., & Trinchieri, G. 1992, ApJS, 80, 531
Fabian, A. C., et al. 1994, PASJ, 46, L59
Fiore, F., Perola, G. C., Matsuoka, M., Yamahuchi, M., & Piro, L. 1992, A&A, 262, 37
George, I. M., Turner, T. J., & Netzer, H. 1995, ApJ, 438, L67
Giommi, P., Beuermann, K., Barr, P., Schwope, A., Tagliaferri, G., & Thomas, H. C. 1989, MNRAS, 236, 375
Gondhalekar, P. M., Kellett, B. J., Pounds, K. A., Matthews, L., & Quenby, J. J. 1994, MNRAS, 268, 973
Guainazzi, M., Matsuoka, M., Piro, L., Mihara, T., & Yamahuchi, M. 1994, ApJ, 436, L35
Halpern, J. P. 1982, Ph.D. thesis, Harvard Univ.

Hayes, M. J. C., Bell Burnell, S. J., Culhane, J. L., Ward, M. J., Barr, P., Ives, J. C., & Sangord, P. W. 1981, Space Sci. Rev., 30, 39
Hayashi, I., Koyama, K., Awaki, H., & Ueno, S. 1996, PASJ, 48, 219
Hewitt, A., & Burbidge, G. 1991, ApJS, 75, 297
Holt, S. S., Mushotzky, R. F., Becker, R. H., Boldt, E. A., Serlemitsos, P. J., Szymkowiak, A. E., & White, N. E. 1980, ApJ, 241, L13
Iwasawa, K. 1994, Ph.D. thesis, Nagoya Univ.
Iwasawa, K., Yaqoob, T., Awaki, H., & Ogasaka, Y. 1994, PASJ, 46, L167
Junkes, N., Zinnecker, H., Hensler, G., Dahlem, M., & Pietsch, W. 1995, A&A, 294, 8
Kaastra, J. K. 1991, A&A, 249, 70
Kirhakos, S. D., & Steiner, J. E. 1990, AJ, 99, 1722
Kolman, M., Halpern, J. P., & Martin, C. 1993, ApJ, 403, 592
Kriss, G. A., et al. 1996, ApJ, 467, 629
Kruper, J., Urry, C. M., & Canizares, C. R. 1990, ApJS, 74, 347
Lawrence, A., & Elvis, M. 1982, ApJ, 246, 410
Leach, C. M., McHardy, I. M., & Papadakis, I. E. 1995, MNRAS, 272, 221
Maccacaro, T., Gioia, I. M., Wolter, A., Zamorani, G., & Stoke, J. T. 1988, ApJ, 326, 680
Madejski, G. M., Done, C., Turner, T. J., Mushotzky, R. F., Serlemitsos, P., Fiore, F., Sikora, M., & Begelman, M. C. 1993, Nature, 365, 626
Madejski, G. M., et al. 1995, ApJ, 438, 672
Maiolino, R., & Rieke, G. H. 1995, ApJ, 454, 95
Makashima, K., et al. 1994, PASJ, 46, L77
Malaguti, G., Bassani, L., & Caroli, E. 1994, ApJS, 94, 517
Marshall, F. E., et al. 1993, ApJ, 405, 168
Matsuoka, M., Piro, L., Yamahuchi, M., & Murakami, T. 1990, ApJ, 361, 440
Mazzarella, J. M., & Boroson, T. A. 1993, ApJS, 85, 27
McLeod, K. K., & Rieke, G. H. 1995, ApJ, 441, 96
Mihara, T., Matsuoka, M., Mushotzky, R. F., Kunieda, H., Otani, C., Miyamoto, S., & Yamauchi, M. 1994, PASJ, 46, L137
Mineo, T., & Stewart, G. C. 1993, MNRAS, 262, 817
Morgan, B., & Kwitter, K. B. 1978, ApJ, 224, L43
Morini, M., Anselmo, F., & Molteni, D. 1989, ApJ, 347, 750
Morse, J. A., Wilson, A. S., Elvis, M., & Weaver, K. A. 1995, ApJ, 439, 121
Mulchaey, J. S., Colbert, E., Wilson, A. S., Mushotzky, R. F., & Weaver, K. A. 1993, ApJ, 414, 144
Mulchaey, J. S., et al. 1994, ApJ, 436, 586
Mulchaey, J. S., Mushotzky, R. F., & Weaver, K. A. 1992, ApJ, 390, L69
Mushotzky, R. F. 1982, ApJ, 256, 92
Mushotzky, R. F., Done, C., & Pounds, K. A. 1993, ARA&A, 31, 717
Mushotzky, R. F., Marshall, F. E., Boldt, E. A., Holt, S. S., & Serlemitsos, P. J. 1980, ApJ, 235, 377
Nandra, K., et al. 1993, MNRAS, 260, 504
Nandra, K., & Pounds, K. A. 1994, MNRAS, 268, 405
Nandra, K., Pounds, K. A., & Stewart, G. C. 1990, MNRAS, 242, 660
Nandra, K., Pounds, K. A., Stewart, G. C., George, I. M. & Hayashida, K. 1991, MNRAS, 248, 760
Osterbrock, D. E., & Martel, A. 1993, ApJ, 414, 552
Otani, C., et al. 1996, PASJ, 48, 2110
Pan, H. C., Stewart, G. C., & Pounds, K. A. 1990, MNRAS, 242, 177
Penston, M. V., & Perez, E. 1984, MNRAS, 211, 33
Petre, R., Mushotzky, R. F., Serlemitsos, P. J., Jahoda, K., & Marshall, F. E. 1993, ApJ, 418, 644
Phillips, M. M., Charles, P. A., & Baldwin, J. A. 1983, ApJ , 266, 485
Piccinotti, G., Mushotzky, R. F., Boldt, E. A., Holt, S. S., Marshall, F. E., Serlemitsos, P. J., & Shafer, A. 1982, ApJ, 253, 485
Pietsch, W., Vogler, A., Kahabka, P, Jain, A., & Klein, U. 1994, A&A, 284, 386
Piro, L., Yamauchi, M., & Matsuoka, M. 1990, ApJ Lett., 360, 35
Pounds, K. A. 1990, MNRAS, 242, 20
Pounds, K. A., Nandra, K., Fink, H. H., & Makino, F. 1994, MNRAS, 267, 193
Ptak, A., Yaqoob, T., Serlemitsos, P. J., Mushotzky, R. F., & Otani, C. 1994, ApJ, 436, 31
Rebecchi, S., Bassani, L., Caroli, E., & Di Cocco, G. 1992, Nuovo Cimento, 15C(5), 889
Reichert, G. A., Mushotzky, R. F., Petre, R., & Holt, S. S. 1985, ApJ, 296, 69
Reynolds, C. S. 1997, MNRAS, in press
Reynolds, C. S., Fabian, A. C. Makashima, K., Fukazawa, Y., & Tamura, T. 1994, MNRAS, 268, L55
Rhee, G., Burns, J. O., & Kowalksi, M. P. 1994, AJ, 108, 1137
Rowan-Robinson, M. 1985, in The Cosmological Distance Ladder, ed. W. H. Freeman (New York: W. H. Freeman), 85
Rudy, R. J. 1984, ApJ, 284, 33
Santos-Lleo, M., Clavel, P., Glass, I. S., Pelat, D., & Reichert, G. 1994, MNRAS, 270, 580
Serlemitsos, P., Yaqoob, T., Ricker, G., Woo, J., Kunieda, H., Terashima, Y., & Iwasawa, K. 1994, PASJ, 46, L43
Siegel, S., & Castellan, N. J., Jr. 1988, Nonparametric Statistics (New York: McGraw-Hill)
Singh, K. P., Rao, A. R., & Vahia, M. N. 1991, ApJ, 377, 417
Smith, D. A., & Done, C. 1996, MNRAS, 280, 355
Stark, A. A., Gammie, C. F., Wilson, R. W., Bally, J., Linke, R., Hailes, C., & Hurwitz, M. 1990, Bell Laboratories H I Survey, privately distributed tape, data obtained from the High Energy Astrophysics Science Archive Research Center
Storchi-Bergmann, T., Kinney, A. L., & Challis, P. 1995, ApJS, 98, 103
Turner, T. J., George, I. M., Madejski, G. M., Kitamoto, S., & Suzuki, T. 1995, ApJ, 445, 660
Turner, T. J., George, I. M., & Mushotzky, R. F. 1993a, ApJ, 412, 72
Turner, T. J., George, I. M., Mushotzky, R. F., & Nandra, K. 1997, ApJ, 475, 118
Turner, T. J., Nandra, K., George, I. M., Fabian, A. C., & Pounds, K. A. 1993b, ApJ, 419, 127
Turner, T. J., et al. 1993c, ApJ, 407, 556
Turner, T. J., & Pounds, K. A. 1989, MNRAS, 240, 833
Turner, T. J., Urry, C. M., & Mushotzky, R. M. 1993d, 418, 653
Turner, T. J., Weaver, K. A., Mushotzky, R. F., Holt, S. S., & Madejski, G. M. 1991, ApJ, 381, 85
Ueno, S., Koyama, K., Awaki, H., Hayashi, I., & Blanco, P.R. 1996, PASJ, 48, 389
Ueno, S., Koyama, K., & Nishida, M. 1994a, ApJ, 431, L1
Ueno, S., Mushotzky, R. F., Koyama, K., Iwasawa, K., Awaki, H., & Hayashi, I. 1994b, PASJ, 46, L71
Ungerechts, H., & Thaddeus, P. 1987, ApJS, 63, 645
Unwin, S. C., Wehrle, A. E., Urry, C. M., Gilmore, D. M., Barton, E. J., Kjerulf, B. C., Zensus, J. A., & Rabaca, C. R. 1994, ApJ, 432, 103
Véron-Cetty, M.P., & Véron, P. 1986, A&AS, 66, 335
Walter, R., & Fink, H. H. 1993, A&A, 274, 105
Ward, M. J., Done, C., Fabian, A. C., Tennant, A. F., & Shafer, R. A. 1988, ApJ, 324, 767
Ward, M. J., Geballe, T., Smith, M., Wade, R., & Williams, P. 1987, ApJ, 316, 138
Warwick, R. S., Pounds, K. A., & Turner, T. J. 1988, MNRAS, 231, 1145
Warwick, R. S., Sembay, S., Yaqoob, T., Makishima, K., Ohashi, T., Tashiro, M., & Kohmura, Y. 1993, MNRAS, 265, 412
Weaver, K. A. 1993, Ph.D. thesis, Univ. of Maryland
Weaver, K. A., Arnaud, K. A., & Mushotzky, R. F. 1995a, ApJ, 447, 121
Weaver, K. A., Mushotzky, R. F., Serlemitsos, P. J., Wilson, A. S., Elvis, M., & Briel, U. 1995b, ApJ, 597
Weaver, K. A., Nousek, J., Yaqoob, T., Mushotzky, R. F., Makino, F., & Otani, C. 1996, ApJ, 458, 160
Weaver, K. A., Yaqoob, T., Holt, S. S., Mushotzky, R. F., Matsuoka, M., & Yamauchi, M. 1994, ApJ, 436, L27
Whittle, M. 1992, ApJS, 79, 49
Wilkes, B. J., Elvis, M., Fiore, F., McDowell, J., Tananbaum, H., & Lawrence, A. 1992, ApJ, 393, L1
Wilkes, B. J., Schmidt, G. D., Smith, P. S., Mathur, S., & McLeod, K. K. 1995, ApJ, 445, 13
Williams, O. R., et al. 1992, ApJ, 389, 157
Worral, D. M. 1989, in Proc. 23d ESLAB Symp. on Two Topics in X-Ray Astronomy (ESA SP-296), ed. J. Hunt & B. Battrick (Noordwijk: ESA), 719
Worral, D. M., & Wilkes, B. J. 1990, ApJ, 360, 396
Yaqoob, T., et al. 1994, PASJ, ApJ, 436, L27
Yaqoob, T., Serlemitsos, P. J., Mushotzky, R. F., Weaver, K. A., Marshall, F. E., & Petre, R. 1993a, ApJ, 418, 638
Yaqoob, T., & Warwick, R. S. 1991, MNRAS, 248, 773
Yaqoob, T., Warwick, R. S., Makino, F., Otani, Y., & Sokoloski, J. 1993b, MNRAS, 262, 435
Yaqoob, T., Warwick, R. S., & Pounds, K. A. 1989, MNRAS, 236, 153

TABLE 6

AGN HIGH-ENERGY SPECTRA CATALOG

Number (1)	Object (2)	References (3)	Instrument (4)	E (5)	Date (ddmmyy) (6)	Γ (7)	$A(\times 0.01)$ (8)			N_H ($\times 10^{21}$) (9)			χ^2_ν (10)	ν (11)	Conf. (12)
1	Mrk 335†	1	*HEAO* 1/A-2	3–40	07 07 78	1.94 0.28 0.17	0.39	...	...	0.40	6.90	0.40	0.90	127	90
		2	*Ginga*/LAC	2–18	03 12 87	2.07 0.32 0.21	0.46	...	...	15.50	11.30	7.80	0.82	23	90
		2	*Ginga*/LAC	2–18	25 11 88	2.13 0.09 0.05	0.99	...	...	<3.10	...	...	0.31	23	90
		3	BBXRT/A0	2–10	05 12 90	1.87 0.32 0.32	0.15	...	...	0.40	...	...	1.08	13	90
		2	*Ginga*/LAC	2–18	22 12 90	2.25 0.07 0.06	0.63	...	...	<1.70	...	...	1.22	23	90
		4	*ROSAT*/PSPC	0.1–2.0	29 06 91	3.10 0.05 0.05	0.13	...	...	0.41	0.02	0.02	1.93	31	90
		2	*Ginga*/LAC	2–18	02 07 91	1.94 0.28 0.17	0.45	...	...	<8.50	...	...	0.90	23	90
2	S5 0014+81	5	*ROSAT*/PSPC	0.1–2.4	16 03 91	2.07 1.20 0.73	0.05	0.03	0.01	1.90	2.40	0.80	1.06	18	68
		5	*ROSAT*/PSPC	0.1–2.4	16 03 91	1.82 0.19 0.19	0.05	0.03	0.03	1.44	...	...	1.02	19	68
		5	*ROSAT*/PSPC	0.1–2.4	16 03 91	1.92 0.67 0.67	0.05	0.02	6e−3	6.40	50	6.40	1.07	18	68
		6	*ASCA*/GIS2	0.8–8	29 10 93	1.69 0.14 0.14	0.06	0.01	0.01	2.20	1.20	1.20	1.35	58	90
		6	*ASCA*/GIS3	0.8–8	29 10 93	1.72 0.13 0.13	0.07	0.01	0.01	2.30	1.20	1.20	0.73	67	90
3	Mrk 348	7	*ROSAT*/PSPC	0.1–2.4	03 01 92	2.40 0.58 0.42	5e−3	9e−4	8e−4	...	...	...	0.6	2	90
4	NGC 526A†	1	*HEAO* 1/A-2	3–40	10 06 78	1.47 0.18 0.17	0.36	...	...	14.80	15.50	12.90	1.33	127	90
		2	*Ginga*/LAC	2–18	15 12 88	1.25 0.12 0.11	0.13	...	...	7.80	6.40	5.80	0.71	23	90
5	Fairall 9	2	*Ginga*/LAC	2–18	22 11 90	1.86 0.03 0.02	1.04	...	...	<1.40	...	...	1.14	23	90
6	Mrk 573	8	*ROSAT*/PSPC	0.1–2	29 01 92	3.50 0.39 0.36	2e−3	...	...	0.45	0.11	0.10	1.23	30	90
7	NGC 985	9	*ROSAT*/PSPC	0.1–2.0	09 08 93	2.58 0.10 0.09	0.36	0.01	0.01	0.31	0.03	0.02	2.57	29	68
8	ESO 198−G24	4	*ROSAT*/PSPC	0.1–2.0	22 11 91	2.28 0.07 0.07	0.55	...	...	0.28	0.02	0.02	2.52	25	90
		4	*ROSAT*/PSPC	0.1–2.0	21 07 92	2.19 0.06 0.06	0.23	...	...	0.23	0.02	0.02	1.07	28	90
9	NGC 1068	10	BBXRT/A0+B0	0.3–10	09 12 90	1.50 0.50 1.25	0.05	...	...	0.31	...	...	...	...	90
		11	*ROSAT*/PSPC	0.1–2.4	SURVEY	2.92 0.39 0.39	0.45	...	...	0.41	0.17	0.17	1.39	16	68
		12	*ASCA*/SIS+GIS	3–10	25 07 93	1.27 0.3 0.3	...	...	...	<50	...	...	...	...	90
10	Mrk 372	8	*ROSAT*/PSPC	0.1–2	15 08 92	2.17 0.15 0.15	0.06	...	...	0.85	0.11	0.09	1.11	54	90
11	NGC 1275	11	*ROSAT*/PSPC	0.1–2.4	SURVEY	1.56 0.57 0.57	15.70	...	...	1.85	0.57	0.57	1.02	31	68
		13	*ROSAT*/PSPC	0.1–2.4	02 02 92	2.79 0.40 0.40	0.16	...	...	4.47	1.17	1.12	1.82	24	90
12	NGC 1365	8	*ROSAT*/PSPC	0.1–2	22 08 92	3.01 0.27 0.27	6e−3	...	...	0.58	0.11	0.10	2.12	37	90
13	NRAO 140	14	*ROSAT*/PSPC	0.1–2.4	08 08 92	2.33 0.95 0.82	2.00	0.2	0.2	3.88	0.95	0.82	1.11	18	90
		14	*ASCA*/SIS+GIS	3–10	01 02 94	1.73 0.03 0.03	0.87	0.09	0.09	2.99	0.20	0.20	0.99	716	90
14	3C 111†	1	*HEAO* 1/A-2	3–40	03 03 78	1.89 0.18 0.17	1.28	...	...	19.40	10.10	9.40	1.24	127	90
		2	*Ginga*/LAC	2–18	04 02 89	1.78 0.04 0.04	1.08	...	...	18.20	2.00	1.80	1.33	23	90
15	3C 120	1	*HEAO* 1/A-2	3–40	07 09 78	1.77 0.09 0.06	0.85	...	...	1.20	2.50	1.20	1.03	127	90
16	PKS 0438−43	5	*ROSAT*/PSPC	0.1–2.4	19 02 91	1.83 0.61 0.35	0.04	8e−3	4e−3	0.86	1.06	0.32	1.10	21	68
		5	*ROSAT*/PSPC	0.1–2.4	19 09 91	1.67 0.38 0.33	0.03	4e−3	3e−3	0.65	0.48	0.22	1.22	21	68
		38	*ASCA*/SIS+GIS	0.1–10	13 07 93	1.80 0.20 0.18	...	...	...	2.02	1.13	0.88	0.93	67	90
17	NGC 1672	15	*Ginga*/LAC	2–10	03 08 91	1.50 0.2 0.2	0.05	...	...	6.31	25.31	0	0.56	23	90
18	NGC 1667	15	*Ginga*/LAC	2–10	16 10 90	1.10 0.5 0.5	0.03	...	...	25.12	74.88	0	0.96	16	90
19	IRAS 04575−7537	32	*Ginga*/LAC	2–10	04 10 90	1.04 0.19 0.08	0.69	...	...	10.5	7.9	2.9	1.06	23	90
20	NGC 1808	15	*Ginga*/LAC	2–10	15 10 90	2.10 0.24 0.24	0.13	...	...	104.7	1.38	1.38	0.94	16	90
		16	*ROSAT*/PSPC	0.1–2.4	18 02 91	7.10 1.10 1.40	2e−5	...	...	9.10	3.20	2.10	1.29	19	68
21	Akn 120†	2	*Ginga*/LAC	2–18	22 09 88	1.82 0.04 0.04	1.11	...	...	<0.90	...	...	1.45	23	90
		17	*ROSAT*/PSPC	0.1–2.4	18 09 92	1.95	0.8	9e−3	9e−3	0.74	0.01	0.01	15.89	14	68

TABLE 6—*Continued*

Number (1)	Object (2)	References (3)	Instrument (4)	E (5)	Date (ddmmyy) (6)	Γ (7)			$A(\times 0.01)$ (8)			N_H ($\times 10^{21}$) (9)			χ^2_ν (10)	ν (11)	Conf. (12)
22	Pic A	11	*ROSAT*/PSPC	0.1–2.4	SURVEY	2.34	0.62	0.62	0.30	...	...	0.68	0.29	0.29	1.41	13	68
23	NGC 2110	1	*HEAO* 1/A-2	3–40	09 10 78	1.81	0.11	0.11	1.45	...	...	67.0	11.0	10.60	1.21	127	90
		2	*Ginga*/LAC	2–18	26 09 89	1.67	0.05	0.04	0.92	...	...	22.8	2.30	2.20	0.63	23	90
		18	BBXRT	0.4–11	06 12 90	1.41	0.50	0.50	0.46	...	...	25.0	5.0	5.0	...	...	90
24	MCG 8-11-11	1	*HEAO* 1/A-2	3–40	05 10 78	1.72	0.11	0.11	0.88	...	...	4.50	5.70	2.50	1.16	127	90
25	Mrk 3	8	*ROSAT*/PSPC	0.1–2	13 03 91	4.58	1.96	1.07	3e−4	...	...	3.10	2.93	1.39	1.41	29	90
		19	*ROSAT*/HRI	0.1–2	12 03 92	4.58	...	...	4e−4	...	...	3.97	...	...	...	...	...
		20	*ASCA*/SIS+GIS	1–10	21 04 93	1.78	0.17	0.15	0.19	...	...	442	135	110	1.57	255	90
26	Mrk 78	8	*ROSAT*/PSPC	0.1–2	15 03 91	2.70	3.98	1.28	1e−3	...	...	0.70	5.76	0.52	1.62	5	90
27	Mrk 79	9	*ROSAT*/PSPC	0.1–2.0	24 09 93	2.57	0.11	0.11	1.03	0.03	0.03	0.75	0.05	0.05	0.84	29	68
28	3C 212	21	*ROSAT*/PSPC	0.1–2	12 05 92	2.4	0.8	0.6	0.03	0.01	0.009	8.70	7.50	6.30	0.72	21	68
29	NGC 2992	1	*HEAO* 1/A-2	3–40	24 05 78	1.71	0.08	0.07	1.94	...	...	4.80 0	4.30	4.10	1.16	127	90
		2	*Ginga*/LAC	2–18	30 04 90	1.64	0.08	0.08	0.40	...	...	13.60	3.30	3.30	1.53	230	90
30	MCG −5-23-16†	1	*HEAO* 1/A-2	3–40	12 05 79	1.75	0.07	0.08	2.14	...	...	5.40	4.60	4.0	1.50	127	90
		2	*Ginga*/LAC	2–18	30 11 88	1.57	0.06	0.05	0.95	...	...	11.50	3.00	2.60	1.30	23	90
		2	*Ginga*/LAC	2–18	05 12 88	1.32	0.10	0.10	0.31	...	...	12.00	5.60	5.80	0.55	23	90
		7	*ROSAT*/PSPC	0.1–2.4	27 11 91	1.56	...	...	1.10	0.37	0.17	13.10	1.60	1.30	1.40	2	90
31	M81	39	BBXRT	0.6–10	05 12 90	2.15	0.13	0.13	0.63	...	...	2.20	0.10	0.50	...	...	90
		11	*ROSAT*/PSPC	0.1–2.4	SURVEY	2.39	0.75	0.75	0.32	...	...	0.87	0.42	0.42	0.49	13	68
32	M82	11	*ROSAT*/PSPC	0.1–2.4	SURVEY	2.05	1.42	1.42	0.74	...	...	1.83	0.29	0.29	1.60	20	68
33	NGC 3227†	1	*HEAO* 1/A-2	3–40	23 11 78	1.33	0.21	0.18	0.23	...	...	11.90	21.50	11.70	1.20	127	90
		2	*Ginga*/LAC	2–18	16 04 88	1.73	0.04	0.03	1.03	...	...	1.40	1.40	1.0	1.54	23	90
		2	*Ginga*/LAC	2–18	09 12 90	1.66	0.04	0.03	0.91	...	...	3.0	1.40	1.20	0.65	23	90
34	IRAS 1040+706	15	*Ginga*/LAC	2–10	18 10 90	1.4	0.06	0.06	0.05	...	...	147.9	1.35	1.35	1.25	12	90
35	NGC 3516†	2	*Ginga*/LAC	2–18	07 10 89	1.74	0.11	0.08	0.86	...	...	48.70	7.70	5.40	2.26	23	90
		2	*Ginga*/LAC	2–18	12 10 89	1.68	0.09	0.09	0.75	...	...	71.90	8.70	8.50	1.33	23	90
		2	*Ginga*/LAC	2–18	19 10 89	1.65	0.14	0.12	0.68	...	...	60.20	11.90	10.10	0.93	23	90
		19	*ROSAT*/HRI	0.1–2	18 04 92	1.60	...	...	0.40	...	...	0.16	...	...	...	...	...
36	NGC 3783	1	*HEAO* 1/A-2	3–40	05 01 78	1.91	0.33	0.26	1.18	...	...	34.20	22.70	18.0	1.11	127	90
		1	*HEAO* 1/A-2	3–40	08 07 78	1.48	0.08	0.05	0.53	...	...	3.70	4.80	2.80	0.89	127	90
		2	*Ginga*/LAC	2–18	13 01 90	1.77	0.03	0.03	1.88	...	...	21.80	1.50	1.40	2.82	23	90
		22	*ROSAT*/PSPC	0.1–2.4	23 07 92	2.35	...	...	0.63	...	...	0.81	...	...	7.09	27	90
		40	*ASCA*/SIS+GIS	3–6	19 12 93	1.39	0.06	0.06	...	...	...	0.85	...	...	0.91	709	90
		40	*ASCA*/SIS+GIG	3–6	23 12 93	1.29	0.06	0.06	...	...	...	0.85	...	...	1.00	709	90
37	NGC 4051†	2	*Ginga*/LAC	2–18	03 06 87	1.63	0.07	0.06	0.36	...	...	<2.60	...	...	1.07	23	90
		2	*Ginga*/LAC	2–18	13 05 88	1.74	0.07	0.05	0.51	...	...	2.80	2.30	1.80	0.98	23	90
		2	*Ginga*/LAC	2–18	21 11 90	1.90	0.15	0.11	0.71	...	...	9.90	5.40	4.40	0.96	23	90
		11	*ROSAT*/PSPC	0.1–2.4	SURVEY	3.21	0.18	0.18	0.44	...	...	0.27	0.05	0.05	1.09	16	68
		23	*ASCA*/SIS+GIS	2.5–6	25 04 93	1.89	0.06	0.06	0.65	...	...	0.13	...	...	...	...	...
38	NGC 4151	1	*HEAO* 1/A-2	3–40	06 12 77	1.49	0.12	0.10	1.77	...	...	112	19	16.80	1.20	127	90
		1	*HEAO* 1/A-2	3–40	... ...	1.50	0.05	0.04	...	...	...	55.70	5.30	4.70	1.64	127	90
		24	*ASCA*/SIS	0.9–10	25 05 93	1.00	0.10	0.10	...	...	...	89	7	7	1.31	416	90
		24	*ASCA*/SIS	0.9–10	05 11 93	1.20	0.10	0.10	...	...	...	21.70	1.30	1.30	1.30	494	90
		19	*ROSAT*/HRI	0.1–2	17 05 93	2.55	...	...	0.10	...	...	0.31	...	...	...	...	...
39	NGC 4258	25	*ROSAT*/PSPC	0.1–2.4	09 05 92	3.70	...	...	6e−3	...	...	0.74	...	...	4.40	...	...
		26	*ASCA*/SIS+GIS	0.5–10	15 05 93	1.78	0.29	0.29	0.18	...	...	150	20	20	0.95	106	90

TABLE 6—*Continued*

Number (1)	Object (2)	References (3)	Instrument (4)	E (5)	Date (ddmmyy) (6)	Γ (7)	$A(\times 0.01)$ (8)		N_H ($\times 10^{21}$) (9)			χ^2_ν (10)	ν (11)	Conf. (12)
40	3C 273	1	*HEAO* 1/A-2	3–40	17 06 78	1.45 0.08 0.06	1.55	...	...	0.30	3.40	0.30	0.94	127	90
		1	*HEAO* 1/A-2	3–40	.....	1.48 0.04 0.03	1.51	...	...	0.30	0.40	0.30	1.40	127	90
		11	*ROSAT*/PSPC	0.1–2.4	SURVEY	2.16 0.13 0.13	1.78	...	...	0.15	0.03	0.03	1.12	...	68
		27	*ROSAT*/PSPC	0.1–2.4	15 12 92	2.13 0.07 0.08	2.34	0.05	0.04	0.13	0.02	0.02	1.75	12	90
		27	*ROSAT*/PSPC	0.1–2.4	18 12 92	2.08 0.08 0.07	2.63	0.04	0.05	0.14	0.02	0.02	1.00	13	90
		27	*ROSAT*/PSPC	0.1–2.4	18 12 92	2.07 0.06 0.05	2.10	0.06	0.05	0.14	0.01	0.01	0.95	22	90
		27	*ROSAT*/PSPC	0.1–2.4	20 12 92	2.13 0.07 0.07	2.36	0.06	0.06	0.15	0.02	0.02	2.00	13	90
		27	*ROSAT*/PSPC	0.1–2.4	22 12 92	2.08 0.07 0.07	1.91	0.05	0.05	0.14	0.02	0.02	1.31	13	90
		27	*ROSAT*/PSPC	0.1–2.4	25 12 92	2.21 0.06 0.07	1.80	0.05	0.04	0.14	0.01	0.01	0.87	16	90
		27	*ROSAT*/PSPC	0.1–2.4	27 12 92	2.23 0.06 0.06	1.85	0.04	0.04	0.15	0.02	0.01	1.47	19	90
		27	*ROSAT*/PSPC	0.1–2.4	29 12 92	2.23 0.06 0.06	1.85	0.04	0.04	0.15	0.02	0.01	1.47	19	90
		27	*ROSAT*/PSPC	0.1–2.4	31 12 92	2.14 0.05 0.05	2.31	0.04	0.04	0.14	0.01	0.01	0.76	33	90
		27	*ROSAT*/PSPC	0.1–2.4	02 01 93	2.14 0.06 0.05	2.00	0.04	0.04	0.14	0.01	0.01	1.43	21	90
		27	*ROSAT*/PSPC	0.1–2.4	03 01 93	2.13 0.06 0.06	1.94	0.04	0.04	0.14	0.01	0.01	1.38	21	90
		27	*ROSAT*/PSPC	0.1–2.4	05 01 93	2.01 0.06 0.05	2.18	0.04	0.04	0.14	0.01	0.01	1.73	22	90
		27	*ROSAT*/PSPC	0.1–2.4	07 01 93	2.08 0.06 0.05	2.34	0.05	0.04	0.16	0.01	0.01	0.56	23	90
		27	*ROSAT*/PSPC	0.1–2.4	09 01 93	2.03 0.05 0.05	2.63	0.04	0.05	0.16	0.01	0.01	1.24	25	90
		28	*ASCA*/SIS	0.4–10	08 06 93	1.60 0.02 0.02	2.66	...	...	0.15	0.05	0.05	1.46	265	90
		28	*ASCA*/SIS	0.4–10	08 06 93	1.66 0.02 0.02	2.83	...	...	0.10	0.05	0.05	1.41	275	90
		28	*ASCA*/GIS	0.8–10	08 06 93	1.61 0.01 0.02	2.32	...	...	<0.06	...	...	1.17	590	90
		28	*ASCA*/GIS	0.8–10	08 06 93	1.63 0.01 0.01	2.46	...	...	<0.05	...	...	1.78	635	90
41	NGC 4593†	29	*EXOSAT*/L+M	2–10	03 02 84	2.10 0.20 0.20	1.50	0.20	0.20	0.37	0.24	0.14	0.22	24	68
		29	*EXOSAT*/L+M	2–10	02 06 84	1.87 0.06 0.06	1.11	0.06	0.06	0.10	0.03	0.03	1.30	30	68
		29	*EXOSAT*/L+M	2–10	01 07 84	1.65 0.09 0.09	1.20	0.10	0.10	0.08	0.04	0.03	0.78	26	68
		29	*EXOSAT*/L+M	2–10	01 07 84	1.75 0.08 0.08	1.22	0.08	0.08	0.09	0.07	0.05	0.80	25	68
		29	*EXOSAT*/L+M	2–10	01 07 84	1.80 0.10 0.10	1.18	0.10	0.10	1.28	2.15	0.80	1.15	25	68
		29	*EXOSAT*/L+M	2–10	25 06 85	1.67 0.10 0.10	0.32	0.02	0.02	0.14	0.05	0.05	1.63	25	68
		29	*EXOSAT*/L+M	2–10	29 06 85	1.60 0.30 0.30	0.34	0.08	0.05	0.08	0.12	0.07	0.89	30	68
		29	*EXOSAT*/L+M	2–10	04 07 85	1.59 0.08 0.08	0.38	0.03	0.03	0.09	0.08	0.05	0.68	25	68
		29	*EXOSAT*/L+M	2–10	09 01 86	1.71 0.04 0.04	0.88	0.03	0.03	0.05	0.01	0.01	1.47	24	68
		2	*Ginga*/LAC	2–18	25 06 87	1.60 0.05 0.03	0.56	...	...	0.20	2.00	0.20	0.77	23	90
		2	*Ginga*/LAC	2–18	13 12 87	1.75 0.04 0.04	0.95	...	...	<1.2	...	...	1.70	23	90
42	3C 279	11	*ROSAT*/PSPC	0.1–2.4	SURVEY	1.65 0.38 0.38	0.68	...	...	0.23	0.11	0.11	0.76	18	68
43	NGC 4945	15	*Ginga*/LAC	2–10	24 07 90	1.7 0.01 0.01	0.01	...	...	14.40	3.60	3.60	1.30	29	90
		15	*Ginga*/LAC	10–30	24 07 90	1.7 0.01 0.01	1.21	...	...	5370	500	500	1.30	29	90
44	MCG −6-30-15†	2	*Ginga*/LAC	2–18	08 09 87	1.72 0.04 0.03	0.95	...	...	4.40	2.0	1.40	3.57	23	90
		2	*Ginga*/LAC	2–18	24 06 89	1.91 0.03 0.02	1.94	...	...	2.10	1.10	0.80	1.06	23	90
		2	*Ginga*/LAC	2–18	01 02 90	1.91 0.02 0.01	2.54	...	...	2.20	0.70	0.50	4.56	23	90
45	NGC 5252	30	*ASCA*/GIS	0.7–10	28 01 94	1.38 0.54 0.23	0.10	...	...	38.10	43.50	33.20	1.00	267	90
		30	*ASCA*/SIS	0.7–10	28 01 94	0.95 1.15 0.75	0.06	...	...	23.40	28.20	19.0	1.38	315	90
46	Mrk 273	8	*ROSAT*/PSPC	0.1–2	19 06 92	3.01 0.75 0.75	1.e−3	...	...	0.55	0.38	0.26	1.16	14	90
47	IC 4329A†	1	*HEAO* 1/A-2	3–40	27 06 78	1.67 0.05 0.05	1.19	...	...	0.50	0.70	0.50	1.19	127	90
		2	*Ginga*/LAC	2–18	08 07 89	1.86 0.01 0.01	4.04	...	...	2.70	0.40	0.50	1.88	23	90
		31	*ROSAT*/PSPC	0.1–2.4	14 01 93	1.15 0.3 0.3	0.90	...	...	2.00	0.30	0.30	1.05	44	90
48	Mrk 279	1	*HEAO* 1/A-2	3–40	... ...	1.58 0.10 10.08	0.24	...	...	0.20	3.70	0.20	1.29	127	90
49	Mrk 464	1	*HEAO* 1/A-2	3–40	09 07 78	1.46 0.11 0.08	0.23	...	...	<4.0	...	...	1.12	127	90

TABLE 6—*Continued*

Number (1)	Object (2)	References (3)	Instrument (4)	E (5)	Date (ddmmyy) (6)	Γ (7)	$A(\times 0.01)$ (8)			N_H ($\times 10^{21}$) (9)			χ^2_ν (10)	ν (11)	Conf. (12)
50	NGC 5506†	1	*HEAO* 1/A-2	3–40	28 06 78	1.68 0.12 0.11	1.19	...	...	29.50	9.0	8.50	1.02	127	90
		2	*Ginga*/LAC	2–18	19 07 88	1.86 0.03 0.02	3.15	...	...	30.70	1.60	1.0	2.85	23	90
		32	*Ginga*/LAC	2–18	06 07 91	1.90 0.03 0.02	0.28	...	...	38.60	2.0	1.40	4.20	24	90
		32	*Ginga*/LAC	2–18	07 07 91	1.80 0.03 0.03	0.21	...	...	36.40	2.0	1.90	4.50	24	90
		32	*Ginga*/LAC	2–18	08 07 91	1.85 0.03 0.03	0.23	...	...	37.10	2.10	2.10	5.50	23	90
		32	*Ginga*/LAC	2–18	09 07 91	1.93 0.02 0.01	0.40	...	...	36.60	1.50	0.90	5.06	24	90
		7	*ROSAT*/PSPC	0.1–2.4	24 01 92	1.84	2.43	0.64	0.49	21.90	2.60	2.40	1.90	2	90
51	NGC 5548†	1	*HEAO* 1/A-2	3–40	... ...	1.77 0.08 0.06	1.37	...	...	0.20	2.10	0.20	1.08	127	90
		2	*Ginga*/LAC	2–18	25 06 88	1.71 0.02 0.02	1.04	...	...	<0.70	...	...	1.40	23	90
		2	*Ginga*/LAC	2–18	09 01 89	1.43 0.10 0.09	0.49	...	...	10.30	4.90	4.20	0.57	23	90
		2	*Ginga*/LAC	2–18	28 01 89	1.57 0.04 0.03	1.05	...	...	4.20	1.50	1.20	1.03	23	90
		2	*Ginga*/LAC	2–18	08 06 89	1.66 0.04 0.04	1.13	...	...	2.30	1.70	1.50	0.57	23	90
		2	*Ginga*/LAC	2–18	13 07 89	1.76 0.03 0.02	1.58	...	...	1.80	1.10	0.90	0.63	23	90
		2	*Ginga*/LAC	2–18	24 05 90	1.72 0.03 0.03	1.09	...	...	0.70	1.0	0.70	1.91	23	90
		2	*Ginga*/LAC	2–18	05 06 90	1.66 0.05 0.03	0.74	...	...	<1.90	...	...	0.89	23	90
		2	*Ginga*/LAC	2–18	12 06 90	1.69 0.02 0.02	1.25	...	...	<0.70	...	...	1.51	23	90
		2	*Ginga*/LAC	2–18	26 06 90	1.59 0.07 0.05	0.52	...	...	0.70	2.60	0.70	0.64	23	90
		2	*Ginga*/LAC	2–18	02 07 90	1.68 0.04 0.03	0.51	...	...	<1.10	...	...	1.12	23	90
		2	*Ginga*/LAC	2–18	08 07 90	1.72 0.07 0.04	0.62	...	...	<2.10	...	...	1.02	23	90
		33	*ROSAT*/PSPC	0.1–2.0	16 07 90	1.98 0.04 0.04	0.47	...	...	0.14	9e−3	9e−3	5.07	24	68
52	NGC 5674	15	*Ginga*/LAC	2–10	18 07 91	1.82 0.15 0.15	0.29	...	...	67.60	1.20	1.20	1.03	24	90
53	Mrk 478	34	*ROSAT*/PSPC	0.11–1.9	19 01 92	3.32 0.25 0.13	0.23	0.01	0.01	0.14	0.02	0.02	...	...	...
54	Mrk 841†	2	*Ginga*/LAC	2–18	23 07 90	1.71 0.18 0.13	0.24	...	...	5.40	6.50	5.10	0.56	23	90
		2	*Ginga*/LAC	2–18	24 01 91	1.62 0.19 0.16	0.18	...	...	<6.30	...	...	0.78	23	90
55	3CR 345	35	*ROSAT*/PSPC	0.1–2.0	19 07 90	1.85 0.22 0.24	...	...	...	0.07	0.05	0.05	1.24	...	90
56	C 34.47	11	*ROSAT*/PSPC	0.1–2.4	SURVEY	2.33 0.30 0.30	0.32	...	...	0.34	0.12	0.12	0.41	13	68
57	NGC 6552	36	*ASCA*/GIS	1–7	PVP	1.80	0.05	...	...	870	180	180	1.01	...	...
58	QSO 1821+643	41	BBXRT	0.5–12	... 12 90	1.77 0.07 0.08	0.51	...	...	0.40	...	...	...	...	90
		11	*ROSAT*/PSPC	0.1–2.4	SURVEY	1.82 0.11 0.11	0.39	...	...	0.20	0.03	0.03	1.31	40	68
59	3C 382†	1	*HEAO* 1/A-2	3–40	23 10 78	1.71 0.14 0.11	0.80	...	...	0.70	0.34	0.70	1.31	127	90
		2	*Ginga*/LAC	2–18	20 07 89	1.57 0.10 0.07	0.28	...	...	1.70	4.0	1.70	0.48	23	90
		2	*Ginga*/LAC	2–18	21 07 89	1.58 0.09 0.07	0.27	...	...	<3.40	...	...	0.36	23	90
		1	*Ginga*/LAC	2–18	22 07 89	1.50 0.05 0.05	0.24	...	...	<1.80	...	...	0.57	23	90
		11	*ROSAT*/PSPC	0.1–2.4	SURVEY	2.65 0.65 0.65	0.16	...	...	0.87	0.31	0.31	0.85	13	68
60	ESO 103−G35	42	*Ginga*/LAC	2–10	24 09 88	1.76 0.19 0.17	1.53	0.77	0.24	176	41	31	0.99	17	90
		32	*Ginga*/LAC	2–18	12 04 91	1.17 0.09 0.09	3.36	...	...	292	25	24	2.69	22	90
61	3C 390.3†	2	*Ginga*/LAC	2–18	11 11 88	1.80 0.01 0.01	1.47	...	...	<0.50	...	...	2.31	23	90
62	ESO 141−G55	1	*HEAO* 1/A-2	3–40	11 04 78	1.67 0.13 0.10	0.79	...	...	<9.60	...	...	1.16	115	90
		4	*ROSAT*/PSPC	0.1–2.0	14 03 91	2.39 0.09 0.09	0.34	...	...	0.55	0.03	0.03	0.71	38	90
63	Cygnus A	37	*Ginga*/LAC	2–10	18 08 91	1.98 0.18 0.20	0.68	...	...	375	75	71	1.14	22	90
64	Mrk 509†	1	*HEAO* 1/A-2	3–40	08 05 78	1.68 0.07 0.05	1.09	...	...	0.40	1.40	0.40	1.20	127	90
		1	*HEAO* 1/A-2	3–40	... ...	1.65 0.03 0.04	1.07	...	...	0.40	0.30	0.40	2.27	127	90
		2	*Ginga*/LAC	2–18	08 10 88	1.86 0.02 0.02	1.91	...	...	<0.40	...	...	4.83	23	90
		2	*Ginga*/LAC	2–18	11 10 88	1.75 0.02 0.02	1.40	...	...	<0.30	...	...	3.34	23	90
		2	*Ginga*/LAC	2–18	18 10 89	1.79 0.02 0.02	1.28	...	...	<0.30	...	...	1.86	23	90
		2	*Ginga*/LAC	2–18	24 10 90	1.75 0.02 0.02	1.40	...	...	<0.30	...	...	1.32	23	90
		4	*ROSAT*/PSPC	0.1–2	10 05 91	2.11 0.13 0.13	0.63	...	...	0.34	0.04	0.04	0.75	16	90

TABLE 6—*Continued*

Number (1)	Object (2)	References (3)	Instrument (4)	E (5)	Date (ddmmyy) (6)	Γ (7)	$A(\times 0.01)$ (8)			N_H ($\times 10^{21}$) (9)			χ^2_ν (10)	ν (11)	Conf. (12)
65	H2106 −099	2	*Ginga*/LAC	2–18	17 05 88	1.84 0.06 0.06	0.42	...	...	<1.20	...	...	1.53	23	90
		2	*Ginga*/LAC	2–18	22 05 88	1.91 0.10 0.08	0.39	...	...	<2.50	...	...	0.51	23	90
66	PKS 2126−158	5	*ROSAT*/PSPC	0.1–2.4	09 05 91	1.52 0.44 0.44	0.10	0.04	0.02	1.10	1.10	0.40	1.37	20	68
		5	*ROSAT*/PSPC	0.1–2.4	12 11 92	1.86 0.72 0.43	0.12	0.06	0.02	1.48	1.32	0.57	0.86	20	68
		38	*ASCA*/SIS+GIS	0.1–10	16 05 93	1.63 0.08 0.09	...	...	...	1.46	0.41	0.37	0.88	249	90
67	NGC 7172	42	*Ginga*/LAC	2–10	26 10 89	1.81 0.07 0.07	2.18	0.34	0 28	97	10	9	0.70	21	90
68	NGC 7213	1	*HEAO* 1/A-2	3–40	26 05 78	1.73 0.11 0.09	1.08	...	...	0.30	1.40	0.30	1.37	127	90
		2	*Ginga*/LAC	2–18	23 06 90	1.70 0.05 0.04	0.87	...	...	0.80	1.80	0.80	1.19	23	90
		2	*Ginga*/LAC	2–18	29 10 90	1.83 0.04 0.04	1.29	...	...	1.50	1.30	1.20	0.90	23	90
69	NGC 7314†	2	*Ginga*/LAC	2–18	27 10 88	1.76 0.06 0.06	0.79	...	...	4.20	2.30	2.20	0.96	23	90
70	Akn 564	9	*ROSAT*/PSPC	0.1–2.0	30 11 93	3.39 0.07 0.07	1.2	0.02	0.02	0.73	0.03	0.03	2.21	29	68
71	NGC 7469†	1	*HEAO* 1/A-2	3–40	01 07 78	1.79 0.09 0.08	0.51	...	...	0.50	1.30	0.50	0.98	127	90
		2	*Ginga*/LAC	2–18	09 07 88	1.85 0.03 0.03	1.17	...	...	<0.70	...	...	2.56	23	90
		4	*ROSAT*/PSPC	0.1–2.0	28 11 91	2.50 0.08 0.08	0.43	...	...	0.56	3e−3	3e−3	2.63	19	90
		11	*ROSAT*/PSPC	0.1–2.4	SURVEY	2.38 0.29 0.29	0.79	...	...	0.51	0.14	0.14	1.26	13	68
		17	*ROSAT*/PSPC	0.1–2.4	02 04 92	2.26 0.05 0.05	0.85	0.01	0.01	0.57	0.02	0.02	1.53	27	68
		43	*ASCA*/SIS	0.57–9	24 11 93	2.02 0.01 0.01	...	...	...	0.53	...	...	1.36	...	90
		43	*ASCA*/GIS	0.8–10	24 11 93	1.97 0.02 0.01	...	...	...	0.53	...	...	1.67	...	90
72	MCG −2-58-22†	1	*HEAO* 1/A-2	3–40	07 06 78	1.62 0.11 0.07	0.93	...	...	0.30	5.40	0.30	1.10	127	90
		2	*Ginga*/LAC	2–18	19 06 89	1.53 0.04 0.04	0.37	...	...	<1.10	...	...	1.15	23	90
		2	*Ginga*/LAC	2–18	05 07 89	1.57 0.11 0.09	0.49	...	...	3.30	4.50	3.30	0.98	23	90
		2	*Ginga*/LAC	2–18	05 11 89	1.46 0.05 0.05	0.31	...	...	<2.40	...	...	0.61	23	90
		2	*Ginga*/LAC	2–18	24 11 89	1.50 0.05 0.05	0.55	...	...	4.10	2.30	2.0	1.59	23	90
		4	*ROSAT*/PSPC	0.1–2.0	21 11 91	2.10 0.07 0.07	0.75	...	...	0.29	0.02	0.02	0.76	21	90
73	NGC 7582	42	*Ginga*/LAC	2–10	25 10 88	1.70	8.30	2.40	1.90	484	254	152	0.66	16	90

NOTE.—See text for explanation of column headings.

REFERENCES.—(1) Weaver, Arnaud, & Mushotzky 1995a; (2) Nandra & Pounds 1994; (3)Turner et al. 1993c; (4)Turner, George, & Mushotzky 1993a; (5)Elvis et al. 1994b; (6)Elvis et al. 1994c; (7) Mulchaey et al. 1993; (8)Turner, Urry, & Mushotzky 1993d; (9) Brandt et al. 1994; (10) Marshall et al. 1993; (11) Brinkmann & Siebert 1994; (12)Ueno et al. 1994b; (13)Rhee, Burns, & Kowalski1994; (14) Turner et al. 1995; (15) Awaki & Koyama 1993; (16) Junkes et al. 1995; (17) Brandt et al. 1993; (18) Weaver 1993; (19) Morse et al. 1995; (20) Iwasawa et al. 1994; (21) Elvis et al. 1994a; (22)Turner et al. 1993b; (23) Mihara et al. 1994; (24) Weaver et al. 1994; (25) Pietsch et al. 1994; (26) Makashima et al. 1994; (27) Leach, McHardy, & Papadakis 1995; (28) Yaqoob et al. 1994; (29) Santos-Lleo et al. 1994; (30) Cappi et al. 1996; (31) Madejski et al. 1995; (32) Smith & Done 1996; (33) Nandra et al. 1993; (34) Gondhalekar et al. 1994; (35) Unwin et al. 1994; (36) Reynolds et al. 1994; (37)Ueno, Koyama, & Nishida 1994a; (38) Serlemitsos et al. 1994; (39) Petre et al. 1993; (40) George, Turner, & Netzer 1995; (41) Yaqoob et al. 1993a; (42) Warwick et al. 1993; (43) Guainazzi et al. 1994.